REPORT DOCUMENTATION PAGE

Form Approved
OMB No. 0704-0188

1. AGENCY USE ONLY (Leave blank)	2. REPORT DATE	3. REPORT TYPE AND DATES COVERED
	5 August 1997	Final, 1 Jan 95 - 30 June 97

4. TITLE AND SUBTITLE
The optical Patch Clamp Stage II: Non-Linear optics as a Probe of Membrane Potential in Living Cells

5. FUNDING NUMBERS
G N00014-95-1-0151

6. AUTHOR(S)
Leslie M. Loew, Ph.D.

7. PERFORMING ORGANIZATION NAME(S) AND ADDRESS(ES)
University of Connecticut Health Center
263 Farmington Avenue
Farmington, CT 06032-3505

8. PERFORMING ORGANIZATION REPORT NUMBER

9. SPONSORING/MONITORING AGENCY NAME(S) AND ADDRESS(ES)
Office of Naval Research, Code 1141SB
800 N. Quincy Street
Arlington, VA 22217

10. SPONSORING/MONITORING AGENCY REPORT NUMBER

11. SUPPLEMENTARY NOTES

12a. DISTRIBUTION/AVAILABILITY STATEMENT
Distribution Unlimited

12b. DISTRIBUTION CODE

13. ABSTRACT *(Maximum 200 words)*

A series of new dyes with superior binding and second harmonic generation (SHG) efficiencies have been synthesized. These dyes are all based on the aminonapthyl-ethenyl-pyridinium chromophore used in our earlier studies of fluorescent potentiometric dyes. We have calibrated the potential-dependent response of the SHG signal on a model membrane system and found the response to be several times more sensitive than the fluorescence signal used most commonly for voltage-sensitive dyes. The utility of the SHG signal for following the membrane potential changes in a system of excitable cells - the visual system of the housefly *Musca domestica* - has been established. This is a particularly appropriate application of the method since the infrared probing light is not absorbed by the photoreceptor cells. A significant enhancement of the SHG signal when the dyes are absorbed to colloidal silver has been demonstrated, suggesting that this approach might be applied to probing the electrical activity of single molecules on a cell surface. Finally, we have obtained the first SHG microscopic images, demonstrating the utility of SHG as a new modality for non-destructive selective contrast in 3D microscopy of living cells.

14. SUBJECT TERMS	15. NUMBER OF PAGES
Second harmonic, membrane potential, microscopy, photoreceptor, dyes	3
	16. PRICE CODE

17. SECURITY CLASSIFICATION OF REPORT	18. SECURITY CLASSIFICATION OF THIS PAGE	19. SECURITY CLASSIFICATION OF ABSTRACT	20. LIMITATION OF ABSTRACT
			SAR

GENERAL INSTRUCTIONS FOR COMPLETING SF 298

The Report Documentation Page (RDP) is used in announcing and cataloging reports. It is important that this information be consistent with the rest of the report, particularly the cover and title page. Instructions for filling in each block of the form follow. It is important to *stay within the lines* to meet *optical scanning requirements*.

Block 1. Agency Use Only *(Leave blank)*.

Block 2. Report Date. Full publication date including day, month, and year, if available (e.g. 1 Jan 88). Must cite at least the year.

Block 3. Type of Report and Dates Covered. State whether report is interim, final, etc. If applicable, enter inclusive report dates (e.g. 10 Jun 87 - 30 Jun 88).

Block 4. Title and Subtitle. A title is taken from the part of the report that provides the most meaningful and complete information. When a report is prepared in more than one volume, repeat the primary title, add volume number, and include subtitle for the specific volume. On classified documents enter the title classification in parentheses.

Block 5. Funding Numbers. To include contract and grant numbers; may include program element number(s), project number(s), task number(s), and work unit number(s). Use the following labels:

C	- Contract	PR	- Project
G	- Grant	TA	- Task
PE	- Program Element	WU	- Work Unit Accession No.

Block 6. Author(s). Name(s) of person(s) responsible for writing the report, performing the research, or credited with the content of the report. If editor or compiler, this should follow the name(s).

Block 7. Performing Organization Name(s) and Address(es). Self-explanatory.

Block 8. Performing Organization Report Number. Enter the unique alphanumeric report number(s) assigned by the organization performing the report.

Block 9. Sponsoring/Monitoring Agency Name(s) and Address(es). Self-explanatory.

Block 10. Sponsoring/Monitoring Agency Report Number. *(If known)*

Block 11. Supplementary Notes. Enter information not included elsewhere such as: Prepared in cooperation with...; Trans. of...; To be published in.... When a report is revised, include a statement whether the new report supersedes or supplements the older report.

Block 12a. Distribution/Availability Statement. Denotes public availability or limitations. Cite any availability to the public. Enter additional limitations or special markings in all capitals (e.g. NOFORN, REL, ITAR).

- DOD - See DoDD 5230.24, "Distribution Statements on Technical Documents."
- DOE - See authorities.
- NASA - See Handbook NHB 2200.2.
- NTIS - Leave blank.

Block 12b. Distribution Code.

- DOD - Leave blank.
- DOE - Enter DOE distribution categories from the Standard Distribution for Unclassified Scientific and Technical Reports.
- NASA - Leave blank.
- NTIS - Leave blank.

Block 13. Abstract. Include a brief *(Maximum 200 words)* factual summary of the most significant information contained in the report.

Block 14. Subject Terms. Keywords or phrases identifying major subjects in the report.

Block 15. Number of Pages. Enter the total number of pages.

Block 16. Price Code. Enter appropriate price code *(NTIS only)*.

Blocks 17. - 19. Security Classifications. Self-explanatory. Enter U.S. Security Classification in accordance with U.S. Security Regulations (i.e., UNCLASSIFIED). If form contains classified information, stamp classification on the top and bottom of the page.

Block 20. Limitation of Abstract. This block must be completed to assign a limitation to the abstract. Enter either UL (unlimited) or SAR (same as report). An entry in this block is necessary if the abstract is to be limited. If blank, the abstract is assumed to be unlimited.

FINAL REPORT

GRANT #: N00014-95-1-151

PRINCIPAL INVESTIGATOR: Dr. Leslie M. Loew

INSTITUTION: University of Connecticut Health Center

GRANT TITLE: The Optical Patch Clamp. Stage II: Non-linear Optics as a Probe of Membrane Potential in Living Cells

AWARD PERIOD: 1 January 1995 - 30 June 1997

OBJECTIVE: To develop new dyes with better non-linear optical properties for staining cell membranes; to measure second harmonic generation (SHG) with the dyes on both artificial and living cell membranes; to use the modulation of the second harmonic signal as a basis for developing high resolution non-linear optical electrophysiological recording methods.

APPROACH: New dyes are synthesized with longer hydrocarbon sidechains to promote stronger binding to cells and with chiral sidechains to optimize SHG. These dyes all contain amino-napthyl-ethenyl-pyridinium (ANEP) chromophores that are known to undergo large charge redistribution upon optical excitation. This is also ideal for SHG. We have recently found that longer chains also retard the rate of flipping across the bilayer; thus, these dyes permit monitoring of potential-dependent signals for longer periods. Dyes are similarly developed for thick tissue preparations, where higher solubility will permit deeper penetration. Also, dyes adsorbed gold and/or silver particles are prepared. The synthetic strategies are based on the well established procedures which have been developed in our laboratory with the key reaction being a Heck coupling reaction. These compounds are tested for non-linear optical effects on the hemispherical bilayer apparatus; as in our previous work, this system can also be used to calibrate the voltage sensitivity of the second harmonic signal. The application of this approach to excitable cells are a primary subject of these investigations. We examine ensembles of cells, such as the photoreceptor from the fly, at low resolution. At high resolution, we are using a femtosecond Titanium-sapphire laser and a scanning microscope to acquire images of SHG signals from the stained membranes of single cells. As a long term goal beyond the award period, we hope to adapt near-field microscopy to be able to study the electrical properties of individual channels with near molecular resolution.

ACCOMPLISHMENTS: We have achieved all of the primary aims of this project. We have synthesized new dyes with better binding and SHG efficiencies. We have calibrated the potential-dependent response of the SHG signal on the hemispherical bilayer apparatus. We have established the utility of the SHG signal for following the membrane potential changes in a system of excitable cells - the visual system of the housefly *Musca domestica*. We have succeeded in demonstrating significant enhancement of the SHG signal when the dyes are adsorbed to colloidal silver. Finally, we have obtained the first SHG microscopic images, demonstrating the utility of SHG as a new modality for non-destructive selective contrast in 3D microscopy of living cells.

A series of dyes containing the ANEP chromophore and a chiral hydrophilic ribosyl group appended to the pyridinium end have been synthesized. The 3 members of this group include compounds with pairs of ethyl, butyl and octyl chains, respectively, appended to the amino terminus. All of theses compunds give large SHG signals when bound to a membrane and in all 3 cases the SHG is strongly modulated by membrane

potential. The shorter chain dye is able to penetrate a complex thick tissue preparation and the longer chain compound is especially suitable for long term experiments because of its resistance to washout.

The *Musca* system is a particularly appropriate system for SHG because the electrical response to stimulation cannot be monitored with standard linear optical recording techniques. This is because the light used for dye absorbance or fluorescence measurements can itself stimulate the physiological response of the photoreceptor cells. In SHG, the incident light is in the infra-red part of the spectrum and therefore does not excite the sensory cells of the visual system. In the experimental setup, the system is illuminated with the 1064nm light of a Q-switched mode locked Nd:YAG laser and the SHG signal at 532nm is monitored with a photomultiplier tube interfaced to a boxcar averager and gated integrator. The physiological response is triggered with the 632 nm line of a HeNe laser focused on the same region of the preparation. The sample is viewed through a surgical microscope equipped with a ccd camera. Stimulation of the photoreceptor cells produces a 25% decrease in the SHG signal which was reversed when the light excitation was discontinued. Comparison to the calibration on the hemispherical bilayer indicates that this corresponds to the expected stimulus-induced depolarization. Interestingly, the adjacent neuronal lamina cells display an increase in SHG upon light-stimulation by a weak set of sequential exposures of the photoreceptor cells. This corresponds to the known hyperpolarization response of these cells expected when photoreceptor excitation is not uniform and synchronous.

Silver dye colloid aggregate (DCA) particles have been produced in solution by adsorption of the chiral dye JPW1234 onto a colloidal silver suspension prepared *in situ.* These DCA in the form of aqueous suspensions and self-assembled colloidal monolayer films were investigated with linear and non-linear spectroscopy, bright/dark field and non-linear light microscopy, and electron microscopy. A strong coupling of localized surface plasmon oscillations with dye absorption observed in the dye stabilized colloidal monolayer films points to a significant degree of electromagnetic dye/colloid interaction. Moreover, the strong nonlinear optical phenomena observed from the DCA both in the aqueous phase and in the form of monolayer colloidal films with moderate intensity infrared illumination at 1.06 m is a result of surface enhancement phenomena in the dye aggregated silver colloids.

Using a Titanium sapphire laser coupled to the scanhead of a confocal microscope, we were able to acquire the first SHG images. These were images of a neuronal cell line stained with JPW2080, the di-octyl version of our ANEP-ribose dye series. This represents a new modality and a new method of contrast for high resolution 3D microscopy. It has all the advantages of 2-photon microscopy with even less phototoxic or photobleaching effects than this already gentle non-linear microscopic technique. As is the case for 2-photon microscopy, SHG microscopy has advantages in depth penetration and photo-damage over confocal microscopy.

CONCLUSIONS: Second harmonic generation has been developed as a tool for high resolution and high sensitivity studies of biological structure and function. This was made possible by combining dye synthesis, laser technology, microscopy and cell biological techniques. The potential of this technology for 3D imaging of live cell physiology has been demonstrated.

SIGNIFICANCE: 1) The idea that chiral aminonaphthyl styryl dyes can be efficient substrates for SHG has been validated. This opens the possibility of a new approach to the development of new classes of organic compounds with vastly improved non-linear optical properties. 2) SHG has been measured for the first time from a dye-stained cell membrane. 3) It has been demonstrated that SHG can be a sensitive probe

of the physiology of a living cell membrane and can have particularly applicability to the study of light-sensitive systems. 4) The dye mediated surface enhancement of nonlinear optical interactions in nanometric DCA delivers sufficient sensitivity to make these particles a potentially new kind of probe of biological structure and function with characteristics that could allow for selective labeling of specific sites in cellular systems; single molecule physiology with optics is a clear possibility. 5) Finally, we have demonstrated a new modality for non-linear microscopy - SHG imaging. This approach is the gentlest yet devised for 3D microscopy of living cells.

PATENT INFORMATION: To date, no patent applications have been filed.

AWARD INFORMATION: Dr. L. Loew, P.I., was appointed Director of the Center for Biomedical Imaging Technology. Dr. A. Lewis, collaborator and consultant on this project was appointed a Fellow of the Royal Society, London.

PUBLICATIONS AND ABSTRACTS:

Ben-Oren, I., G. Peleg, A. Lewis, B. Minke, and L. M. Loew. 1996. Infrared nonlinear optical measurements of membrane potential in photoreceptor cells. *Biophys. J.* 71:1616-1620.

Bouevitch, O., A. Lewis, I. Pinevsky, J. P. Wuskell, and L. M. Loew. 1993. Probing membrane potential with non-linear optics. *Biophys. J.* 65:672-679.

Loew, L. M. 1996a. Potentiometric dyes: imaging electrical activity of cell membranes. *Pure & Appl. Chem.* 68:1405-1409.

Loew, L. M. 1996b. Potentiometric dyes: new modalities for optical imaging of membrane potential. *In* Proceedings of Optical Diagnostics of Living Cells and Biofluids. Vol. 2678. D. L. Farkas and B. J. Tromberg, editors. SPIE, San Jose. 80-87.

Peleg, G., A. Lewis, O. Bouevitch, L. M. Loew, D. Parnas, and M. Linial. 1996. Gigantic optical non-linearities from nanoparticle enhanced molecular probes with potential for selectively imaging the structure and physiology of nanometric regions in cellular systems. *Bioimaging* 4:215-224.

Bouevitch, O., A. Lewis, and L. M. Loew. (1996) Naonoantennae equipped molecular probes: a new approach to non-linear optical microprobing of biosystems. Abstract presented Feb. 21, 1996 Annual Meeting of the Biophysical Society, *Biophys. J.* **70**, A431.

Pure & Appl. Chem., Vol. 68, No. 7, pp. 1405–1409, 1996.
Printed in Great Britain.

Potentiometric dyes: Imaging electrical activity of cell membranes

Leslie M. Loew

Department of Physiology, University of Connecticut Health Center, Farmington, CT 06030 USA

Abstract. Voltage sensitive dyes offer the opportunity to monitor neuronal electrical activity where microelectrode measurements are unsuitable or inadequate. This technology is especially powerful for the study of patterns of activity in complex multicellular preparations. It also makes possible the measurement of spatial and temporal variations in membrane potential along the surface of single cells. The fast dyes which have been developed in this laboratory are in the structural class called styryl or naphthylstyryl. These are amphiphilic membrane staining dyes which usually have a pair of hydrocarbon chains acting as membrane anchors and a hydrophilic group which aligns the chromophore perpendicular to the membrane/aqueous interface. The chromophore is believed to undergo a large electronic charge shift as a result of excitation from the ground to the excited state and this underlies the putative electrochromic mechanism for the sensitivity of these dyes to membrane potential. We have used these dyes to map the membrane potential along the surface of single cells with high resolution digital imaging microscopy techniques. These compounds also display remarkable efficiencies for second harmonic generation. Further, the second harmonic signal can be generated from a dye-stained membrane and is modulatable by changing the membrane voltage.

The development of potentiometric dyes has been motivated by the needs of neuroscientists to monitor neuronal electrical activity where microelectrode measurements are unsuitable or inadequate. This technology is especially powerful for the study of patterns of activity in complex multicellular preparations. It also makes possible the measurement of spatial and temporal variations in membrane potential along the surface of single cells. The dye technology may be suitable for suitable for other applications including photonics and laser technology and it is hoped that this paper will bring the availability of these compounds to the attention of a broader scientific audience.

Many of the fast dyes which have been developed in this laboratory are in the structural class called styryl or naphthylstyryl. These are amphiphilic membrane staining dyes which usually have a pair of hydrocarbon chains acting as membrane anchors and a hydrophilic group which aligns the chromophore perpendicular to the membrane/aqueous interface. The chromophore is believed to undergo a large electronic charge shift as a result of excitation from the ground to the excited state and this underlies the putative electrochromic mechanism for the sensitivity of these dyes to membrane potential (1,2).

The concept of electrochromism and how it can lead to a potentiometric dye is illustrated in Figure 1. According to our molecular orbital calculations (3,4) the naphthylstyryl pyridinium chromophore has most of its positive charge localized near the pyridinium nitrogen in the ground state and near the arylamino nitrogen in the excited state. When a hydrophilic moiety is attached to one end and a pair of hydrocarbon chains to the other, as illustrated for the dye di-4-ANEPPS, the molecule intercalates readily among the amphiphilic lipid molecules in a biological membrane and the chromophore is oriented perpendicular to the membrane surface. This orientation assures that the excitation induced charge redistribution will occur parallel to the electric field within the membrane. A change in the voltage across the membrane will therefore cause a spectral shift resulting from a direct interaction

between the field and the ground and excited state dipole moments. The electric fields in a membrane amount to ca. 10^5 V/cm and the difference between ground and excited state dipoles is about 15 Debye. The result is a shift in the absorbance or fluorescence spectra of just a few nm. But this has been sufficient for many applications of the dyes to biological problems.

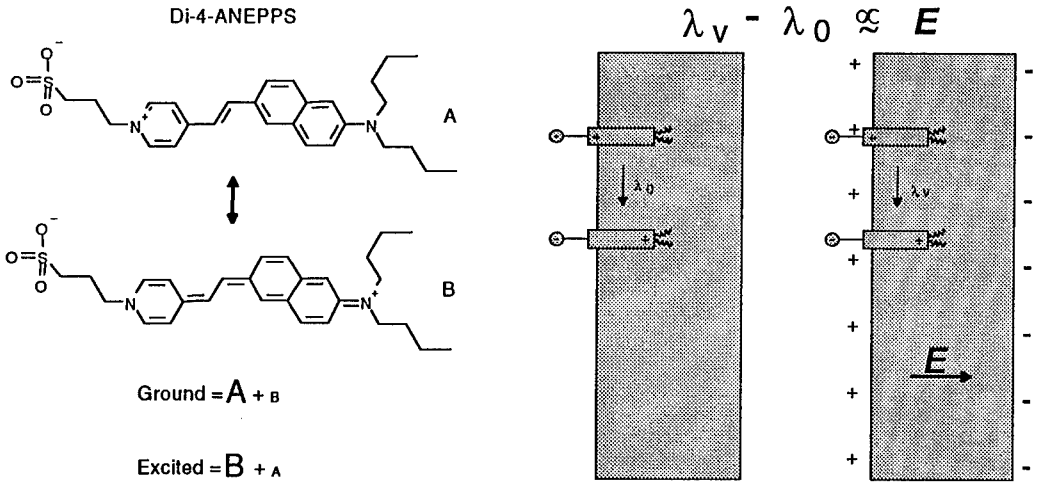

Figure 1. Principals for the design of an electrochromic dye for sensing membrane potential. The chromophore undergoes a large change in dipole moment upon excitation. It is oriented in the membrane so that this changing dipole is parallel to the intramembrane electric field.

It is important to understand that the diverse biological preparations and applications of the potentiometric dye technology require a large repertoire of dyes tailored to each preparation and experimental protocol. We had originally hoped that it might be possible to design a universal potentiometric dye (3) and this goal has been partially realized with the compound di-4-ANEPPS (5). However, it has become clear that the variable physical/chemical characteristics of biological preparations and the optical instrumentation used to study them in different laboratories have belied the practicality of this goal. A large number of dyes have been synthesized in this laboratory (6,7) as well as in the laboratories of Alan Waggoner and Amiram Grinvald (8-11); many of these are commercially available, mainly through Molecular Probes, Inc. There is a continuing need, however, to customize fast potentiometric dyes to the needs of individual experiments. It also follows that it is necessary to have an appreciation of the physical/chemical properties of the existing dyes in order to properly choose and use them for multisite optical recording or digital imaging experiments. Table 1 depicts some of the variations on the naphthylstyryl dyes that have been designed to meet specific needs.

In general, the sensitivities of a potentiometric dye to changes in membrane potential varies from preparation to preparation. For dyes with potential-dependent absorbance changes, the magnitude of the relative change in the optical signal depends on the degree of staining and the thickness of the preparation, so it is difficult to devise a figure of merit. The situation is somewhat better for fluorescence since the entire optical signal usually arises from stained membrane and a relative change may be more meaningful; but even for fluorescence, the signal may be contaminated by fluorescence from non-excitable cells that have been also stained in the preparation. L.B. Cohen has suggested the signal to noise ratio (S:N) in the squid axon preparation as a means to compare the sensitivities of different dyes. His laboratory has published data on S:N ratios for over 1000 dyes (12-14). In this laboratory, we screen all newly synthesized dyes on a voltage-clamped model membrane and determine both the relative change in transmitted light and fluorescence for a 100 mV step (2,15). The best fast fluorescent dyes show relative changes of ca. 10% for a 100 mV potential step. In general, there is a good correlation between the S:N on the squid axon and the corresponding relative change on the model membrane but some dyes show totally different behavior in the 2 systems (16); this was traced to differences in the dye's ability to permeate through the glia surrounding the axon and to the ability of some dyes to flip across the axon membrane but not that of the model membrane.

Table 1. Properties of Selected Potentiometric Dyes

Name	Other Names	Comments	ABS (nm)	EM (nm)	Structure
JPW-211	Di-4-ANEPPS	Versatile fast dye. May need Pluronic F127 to solubilize. Obtain from Molecular Probes, Inc.	502	723	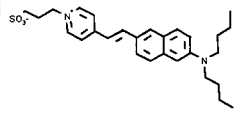
JPW-1114	Di-2-ANEPEQ	More soluble analog of di-4-ANEPPS. Best potentiometric dye for microinjection. Will also show great tissue penetration when applied externally, but may wash out quickly.	529	725	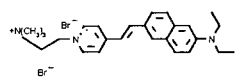
JPW-1153	Di-8-ANEPPS	More slowly internalized than di-4-ANEPPS. Needs Pluronic to stain. Wash away with pluronic then pluronic-free buffer.	500	705	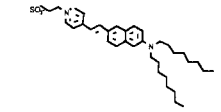
JPW 1259		Chiral ribose group enhances non-linear optical properties in oriented assemblies.	502	712	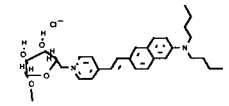
JPW-1294	Di-4-ANEPPQ	Doubly cationic relative of di-4-ANEPPS. Good tissue penetration for thick preparations.	514	715	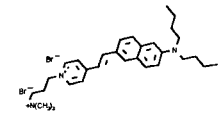
JPW-2045	Di-8-ANEPPQ	Potentiometric dye for neuronal tracing and long-term studies.	513	717	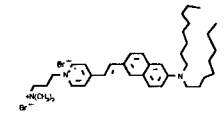
JPW-2066	Di-18:2-ANEPPS	di-linoleyl-ANEPPS, oil soluble. May be microinjected to stain er (ala Mark Terasaki). Potential-dependence not yet established experimentally, but it should work based on precedent.	497	707	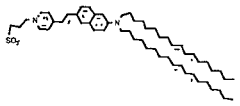

The dye that has been the most popular is di-4-ANEPPS (Figure 1 and Table 1). We recommend that investigators use this compound as a first try because it gives the most consistent results with good sensitivity. In our own work (5,17,18) it was demonstrated that this compound can measure membrane potential in squid axon, red blood cells, guinea pig and sheep heart, lipid vesicles, and a variety of cells in culture (others have published papers employing this dye in at least 10 additional preparations). We have also used this dye to establish the method of dual wavelength ratiometric potential measurements (18). This idea is based on the potential-dependent spectral shift of the ANEP chromophore (15). It gives the same advantages as the more familiar ratiometric dyes for calcium, obviating problems of variable staining and dye bleaching. Most importantly, it permits the imaging of variations in electrical potential laterally along the surface of a single cell (19).

A problem with di-4-ANEPPS is that for some cells it can become rapidly internalized. If the dye lines the inner and outer leaflets of the membrane bilayer, the response to voltage will cancel out. This is a good example of how an experimental difficulty prompted a redesigned fluorescent probe. We discovered that dyes with longer hydrocarbon tails (counterintuitively) are less likely to flip across the bilayer and become internalized. We therefore synthesized di-8-ANEPPS, which contains 2 octyl chains

instead of the butyl chains on di-4-ANEPPS. It is poorly soluble in water so staining of cells requires Pluronic F127, a macromolecular surfactant. Di-8-ANEPPS is now also commercially available and has been employed to follow membrane potentials over long timecourses. It can also be used for ratiometric imaging (19,20).

Of course, other applications are not compatible with the low solubility of either di-4- or di-8-ANEPPS. In a collaboration with Dejan Zecevic of the University of Zagreb, which calls for intracellular injection to label a single neuron in a complex preparation, a dye was required which has high water solubility to minimize injection volume (the solubility of di-4-ANEPPS is only 0.3 μM), will remain internalized, and still have sufficient membrane affinity to bind to the cytosolic face of the plasma membrane. The answer (21) was di-2-ANEPEQ, which contains a pair of ethyl chains at one end and a double positive charge at the other.

We have also prepared indicators with very long hydrocarbon chains for investigators wishing to combine potentiometric studies with neuronal tracing; the dye is applied to one end of a neuron and its water-insolubility prevents it from spreading anywhere but along the membrane of that one cell. In Table 1, di-8-ANEPPQ is an example of such a dye. In addition to the long hydrocarbon chains, the opposite end of the molecule contains a doubly positive charge to inhibit flipping of the dye through the membrane bilayer. This is of great concern because of the very long durations of neuronal tracing experiments.

The dyes may be used to image variations in the electrical properties along the surface of a cell membrane by using them in conjunction with digital fluorescence microscopy. The challenge is to find a way to correct or normalize away contributions to the fluorescence signal resulting from variations in the concentration of dye or the complex morphology of the cell surface and thereby extracting the dyes's response to its electrical environment. This is achieved by employing a dual wavelength ratiometric scheme (18) that is most easily understood by reference to Figure 2. Because the spectrum undergoes a

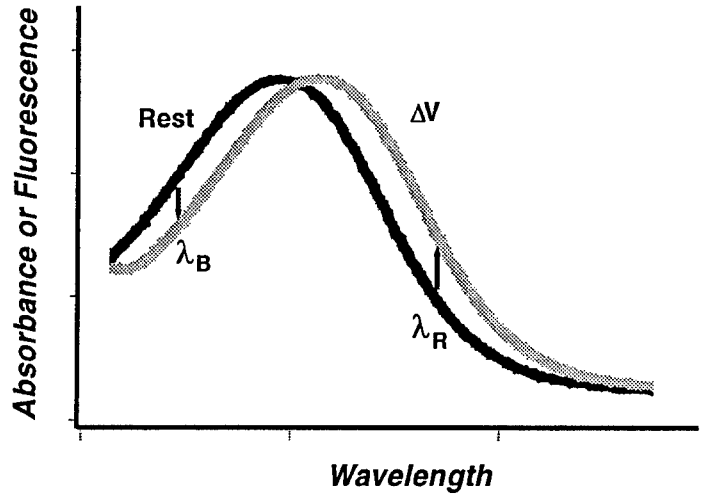

Figure 2.The spectra of styryl dyes are shifted in the presence of electric fields comparable to those found in biological membranes. By ratioing the fluorescence at the red and blue wings of the spectrum, the membrane potential may be monitored without regard to uneven dye distribution.

shift, the fluorescence goes down on the blue wing of the spectrum and up on the red wing. Any variation in concentration or volume dye would cause changes in the same direction at both wavelengths. So a ratio of the two wavelengths normalizes away everything but the dye's response to the intramembrane electric field. This idea was used to study the electric field induced variations in cell membrane potential (19) and allowed us to discover intrinsic variations in intramembrane electric field in different regions of a differentiated neuronal cell (22).

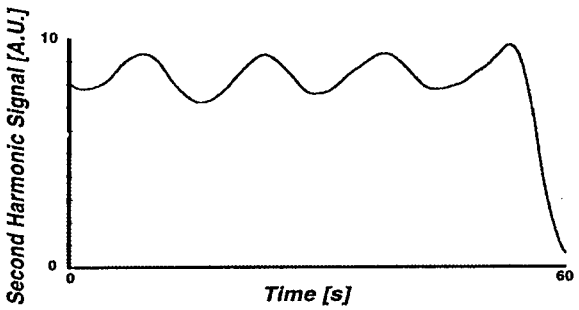

Figure 3. Modulation of SHG Signal from a JPW1259-Stained Lipid Bilayer by 60mV Membrane Potentials. Square wave pulses are applied with periods of 8s at +30mV and 8s at -30 mV. The time course of the optical response is distorted by the timeconstant of the electronics. The experiment is described in Bouevitch et al. (1993) Biophys. J. 65:672-679.

Finally, one of the most exciting findings has been that these dyes all display significant non-linear optical properties when deposited as monolayers (23) or when bound to one surface of a biological membrane (24). The best of the dyes for this purpose is JPW1259 (Table 1) which has a chiral sugar moiety appended to the pyridinium nitrogen. Furthermore, the second harmonic signal displayed by these dyes is itself sensitive to membrane potential. Figure 3 illustrates the voltage-dependent modulation of the second harmonic signal from a model lipid bilayer membrane stained with JPW1259,; details may be found in Bouevitch et al., 1993 (24). The amplitude of the modulation is linearly dependent on the membrane potential and in unpublished work with the laboratory of A. Lewis, we have shown that physiological responses from living cells can be monitored with this technique.

ACKNOWLEDGEMENT

I would like to thank all my colleagues who have collaborated with me over the past ten years. The names are included among the references listed at the end of the paper. Also, I would like to acknowledge the financial support of the National Institute of General Medical Sciences and the Office of Naval Research.

REFERENCES

1. L. M. Loew *et al.*, *Nature* **281**, 497 (1979).
2. L. M. Loew and L. Simpson, *Biophys. J.* **34**, 353 (1981).
3. L. M. Loew, G. W. Bonneville, J. Surow, *Biochemistry* **17**, 4065 (1978).
4. L. M. Loew in *Spectroscopic Membrane Probes,* L. M. Loew, Ed. (CRC Press, Boca Raton, FL, 1988), vol. II, pp. 139-152.
5. L. M. Loew *et al.*, *J. Membr. Biol.* **130**, 1 (1992).
6. A. Hassner, D. Birnbaum, L. M. Loew, *J. Org. Chem.* **49**, 2546 (1984).
7. B. Ehrenberg *et al.*, *Biophys. J.* **53**, 785 (1988).
8. A. S. Waggoner, *Ann. Rev. Biophys. Bioeng.* **8**, 847 (1979).
9. A. S. Waggoner, in *The Enzymes of Biological Membranes*, A. N. Martonosi, Ed. (Plenum, New York, 1985), pp. 313-331.
10. A. S. Grinvald *et al.*, *Biophys. J.* **39**, 301 (1982).
11. A. Grinvald *et al.*, *Biophys. J.* **42**, 195 (1983).
12. L. B. Cohen *et al.*, *J. Membr. Biol.* **19**, 1 (1974).
13. W. N. Ross *et al.*, *J. Membr. Biol.* **33**, 141 (1977).
14. R. K. Gupta *et al.*, *J. Membr. Biol.* **58**, 123 (1981).
15. E. Fluhler, V. G. Burnham, L. M. Loew, *Biochemistry* **24**, 5749 (1985).
16. L. M. Loew *et al.*, *Biophys. J.* **47**, 71 (1985).
17. D. Gross and L. M. Loew, in *Methods in Cell Biology*, vol. 30, Y. Wang and D. L. Taylor, Ed. (Academic Press, New York, 1989), pp. 193-218.
18. V. Montana, D. L. Farkas, L. M. Loew, *Biochemistry* **28**, 4536 (1989).
19. R. S. Bedlack, M.-d Wei, L. M. Loew, *Neuron* **9**, 393 (1992).
20. E. Gross, R. S. Bedlack, L. M. Loew, *Biophys. J.* **67**, 208 (1994).
21. S. Antic *et al.*, *Biological Bulletin* **183**, 350 (1992).
22. R. S. Bedlack *et al.*, *Neuron* **13**, 1187 (1994).
23. J. Y. Huang, A. Lewis, L. M. Loew, *Biophys. J.* **53**, 665 (1988).
24. O. Bouevitch *et al.*, *Biophys. J.* **65**, 672 (1993).

REPRINT

SPIE—The International Society for Optical Engineering

Reprinted from

Proceedings of

Optical Diagnostics of Living Cells and Biofluids

28 January–1 February 1996
San Jose, California

Volume 2678

Invited Paper

Potentiometric dyes: new modalities for optical imaging of membrane potential

Leslie M. Loew

Department of Physiology and Center for Biomedical Imaging Technology, University of Connecticut Health Center, Farmington, CT 06030.

ABSTRACT

Voltage sensitive dyes permit the measurement of biomembrane electrical activity where microelectrode measurements are unsuitable or inadequate. This laboratory has developed 2 classes of such dyes as well as some new optical methods for mapping membrane potential in single cells. One class of compounds consists of amphiphilic membrane staining dyes containing a putative electrochromic chromophore aligned perpendicular to the membrane/aqueous interface. We have used these dyes to map the membrane potential along the surface of single cells with high resolution dual wavelength ratiometric imaging microscopy techniques. We have found intrinsic regional variations in the electrical properties of cell membranes. Adding chirality produces compounds that display remarkable efficiencies for second harmonic generation. Further, the second harmonic signal can be generated from a dye-stained membrane and is modulatable by changing the membrane voltage. This can form the basis for measurements of membrane electrophysiology at high 3D resolution with infrared light. A second class of dyes are membrane-permeant cations which act as Nernstian indicators. We have developed calibration methods which allow the use of these compounds to quantitate the membrane potential of individual mitochondria from confocal or widefield images of living cells.

KEYWORDS: membrane potential, fluorescence, dye, imaging, microscopy, mitochondria, confocal, non-linear optics

1. INTRODUCTION

This laboratory has been engaged in the design and synthesis of voltages sensitive dyes for almost 20 years.[1-3] Potentiometric dyes are designed to either measure membrane potentials in cell populations with a macroscopic system such as a spectrofluorometer or to be used in conjunction with a microscope to measure voltages associated with individual cells or organelles. The latter kinds of applications are the primary interest of this laboratory and have directed the dye chemistry development. Such experiments have been of great utility to neuroscientists interested in mapping patterns of electrical activity in complex neuronal preparations with numerous examples spanning the past 15 years.[4-6] In addition, the dyes have been used to map the spatial[7-9] and temporal[10, 11] patterns of electical activity along single cell membranes and have measured potentials in fine processes and at synapses.[12] Recently, we have even been able to measure the membrane potentials across the inner membranes of individual mitochondria within a single living cell.[13] All of these experiments could not be accomplished with conventional electrical measurements using microelectrode or patch clamp techniques. Indeed, the optical techniques offer paths to new insights on cellular and intracellular physiological mechanisms.

The availability of highly sensitive imaging technologies such as low-light level video, laser scanning confocal microscopy, cooled charge coupled device cameras and fast photodiode arrays has tremendously expanded the opportunities for implementation of optical electrophysiological approaches. These detection systems have further partnered with ever expanding available computational power to obviate the processing, analysis and display of the huge volume of image data that is typically acquired in an experiment. The third critical component is the dye chemistry which is required not only for improved sensitivity but also to provide customized potentiometric indicators for specific biological preparations and experimental applications.

In this paper, I will describe 3 new techniques for potentiometric dye measurements that have been developed by myself and my collaborators. The first of these is a ratiometric dual wavelength imaging method that permits us to map electrical potentials along the surface of single cells. The second takes advantage of the non-linear optical properties of some of the dyes to permit membrane potential measurements with near infrared laser light. The third uses a membrane permeant cationic dye to measure the Nernstian distribution of fluorescence across the membrane; using quantitative 3D digital microscopy, we have been able to measure the potential across the membrane of individual mitochondria as well as the plasma membrane. These methods depend on the unique chemical and spectroscopic properties of the organic dyes that were developed for these applications. The considerations that were involved in designing the dyes will therefore also be highlighted.

0-8194-2052-2/96/$6.00

Di-n-ANEPPS

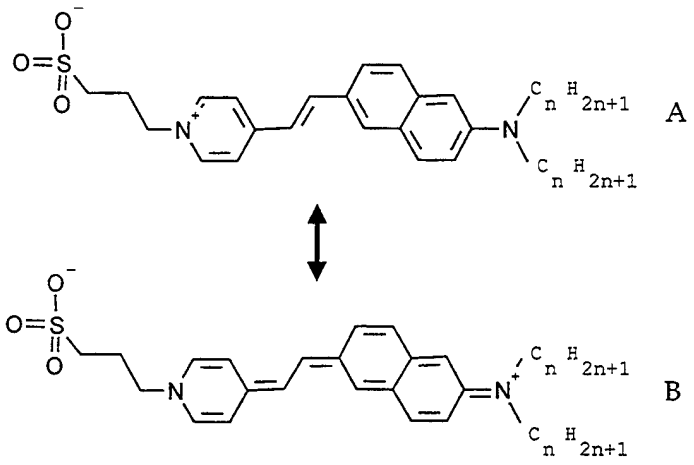

Ground = A + B

Excited = B + A

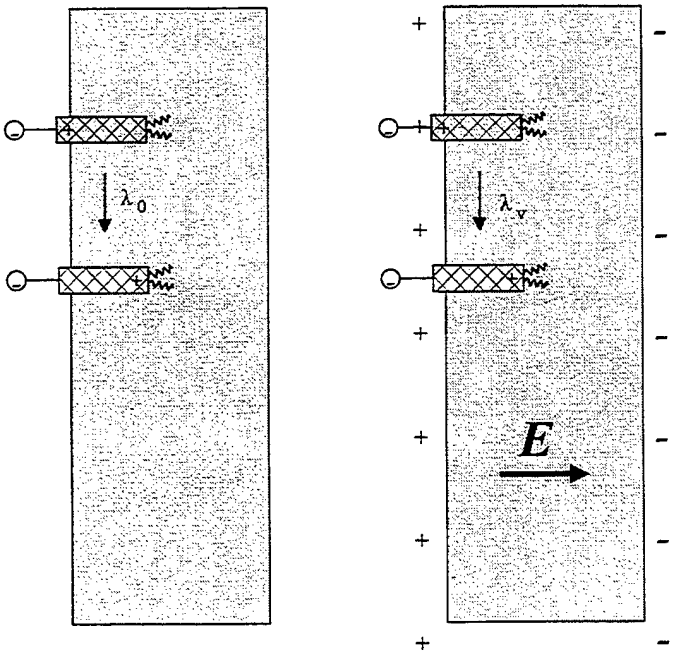

$$\lambda_v - \lambda_0 \propto E$$

Figure 1. Design of an electrochromic dye for sensing membrane potential. The chromophore undergoes a large change in dipole moment upon excitation. It is oriented in the membrane so that this changing dipole is parallel to the intramembrane electric field. A number of dyes have been prepared with variable numbers, n, of carbons in the hydrocarbon chains attached to the amino nitrogen.

2. RATIOMETRIC MAPS OF ELECTRICAL POTENTIALS ALONG CELL SURFACES

2.1 Design of fast charge-shift dyes

Many of the fast dyes which have been developed in this laboratory are in the structural class called styryl or naphthylstyryl. These are amphiphilic membrane staining dyes which usually have a pair of hydrocarbon chains acting as membrane anchors and a hydrophilic group which aligns the chromophore perpendicular to the membrane/aqueous interface. The chromophore is believed to undergo a large electronic charge shift as a result of excitation from the ground to the excited state and this underlies the putative electrochromic mechanism for the sensitivity of these dyes to membrane potential.[1, 14]

The concept of electrochromism and how it can lead to a potentiometric dye is illustrated in Figure 1. According to our molecular orbital calculations[3, 15] the naphthylstyryl pyridinium chromophore has most of its positive charge localized near the pyridinium nitrogen in the ground state and near the arylamino nitrogen in the excited state. When a hydrophilic moiety is attached to one end and a pair of hydrocarbon chains to the other, as illustrated for the dye di-4-ANEPPS, the molecule intercalates readily among the amphiphilic lipid molecules in a biological membrane and the chromophore is oriented perpendicular to the membrane surface. This orientation assures that the excitation induced charge redistribution will occur parallel to the electric field within the membrane. A change in the voltage across the membrane will therefore cause a spectral shift resulting from a direct interaction between the field and the ground and excited state dipole moments. The electric fields in a membrane amount to ca. 10^5 V/cm and the difference between ground and excited state dipoles is about 15 Debye. The result is a shift in the absorbance or fluorescence spectra of just a few nm. But this has been sufficient for many applications of the dyes to biological problems.

2.2 The principle of ratiometric dual wavelength imaging

The dyes may be used to image variations in the electrical properties along the surface of a cell membrane by using them in conjunction with digital fluorescence microscopy. The challenge is to find a way to correct or normalize away contributions to the fluorescence signal resulting from variations in the concentration of dye or the complex morphology of the cell surface and thereby extracting the dye's response to its electrical environment. This is achieved by employing a dual wavelength ratiometric scheme[16] that is most easily understood by reference to Figure 2. Because the spectrum undergoes a shift, the fluorescence goes down on the blue wing of the spectrum and up on the red wing. Any variation in concentration or volume dye would cause changes in the same direction at both wavelengths. So a ratio of the two wavelengths normalizes away everything but the dye's response to the intramembrane electric field.

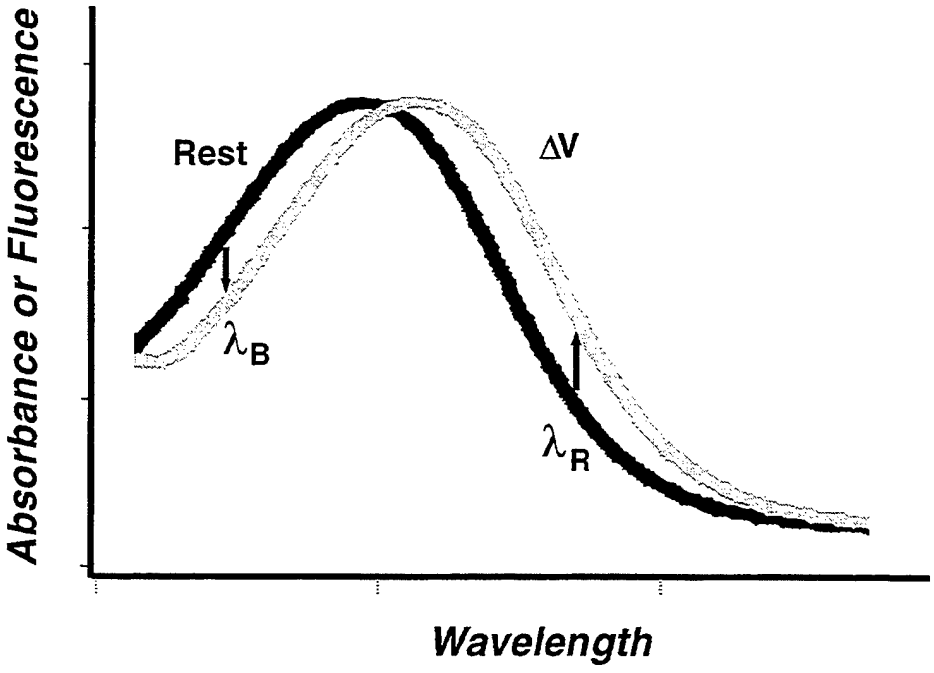

Figure 2.The spectra of styryl dyes are shifted in the presence of electric fields comparable to those found in biological membranes. By ratioing the fluorescence at the red and blue wings of the spectrum, the membrane potential may be monitored without regard to uneven dye distribution.

2.3 Measurement of variations in intramembrane electric field along the surface of a neuronal cell

This idea was used to study the electric field induced variations in cell membrane potential.[8] In this study of electric field induced neurite outgrowth in N1E-115 neuroblastoma cells, it was found that a localized intracellular calcium increase immediately followed the onset of the field and was directly related to the growth response. The presence of voltage sensitive Ca channels in the membranes of these cells suggested that a localized membrane depolarization could lead to the observed intracellular calcium rise via influx from the external medium. The cells were stained with d-8-ANEPPS, a naphthyl styryl dye with 2 octyl chains; the long carbon chains retard the internalization of the dye and permit longer term experiments. Dual wavelength images were acquired and ratio images calculated before during and after exposure to the external electric field stimulus. The experiments showed a cathode-localized depolarization of sufficient magnitude to account for the intracellular calcium increase. The depolarization lasted throughout the application of the electric field. The magnitude of the effect had a dependence on the orientation of the cell with respect to the field; neurites oriented perpendicular to the field direction showed weaker depolarizations than neurites oriented parallel to the field.

A second very exciting finding was that an intrinsic regional variation in dye ratio was found in these neuronal cells. It appeared that the neurites and growth cones of these cells are depolarized relative to the somata.[9] This effect originates from a significant gradient in intramemebrane electric field that we ascribed to dipole potential differences between these regions. The dipole potential, in turn, has its source in the alligned dipoles of the lipid molecules comprising the membrane.[17, 18] Although dipole potentials are large, they drop only over a small depth within the membrane, but this is precisely the location of the probe chromophore. This gradient in dipole potential could have great significance if the electrophysiology of voltage dependent channels is differentially affected in the 2 regions of the cell. Preliminary results from patch clamp studies in this laboratory have shown that the sodium channel in these cells does, indeed display an offset in its voltage dependent activation rate corresponding to an increment of excitability in the growth cone compared to the soma. This could contribute a new mechanism for the diversity of ion channels at a functional rather than a molecular level.

3. MEMBRANE POTENTIAL CAN MODULATE THE NON-LINEAR OPTICAL SIGNALS FROM POTENTIOMETRIC DYES

Several years ago we determined that the styryl and naphthylstyryl dyes can display huge non-linear optical properties when deposited as monolayers, specifically with respect to second harmonic generation (SHG).[19] This is not terribly surprising in that the requirements for SHG include a large second order hyperpolarizability - met by the large electronic redistribution in the excited state relative to the ground state. The requirement for a non-centrosymmetric macroscopic assembly of the molecules is met by the monolayer. It was felt that naphthylstyryl dyes with better efficiencies for SHG could be produced by covalently appending chiral groups to the chromophore. If these dyes were sufficiently active as non-linear optical mediators, SHG signals might even be obtainable from stained membranes and these signals could be sensitive to membrane potential.

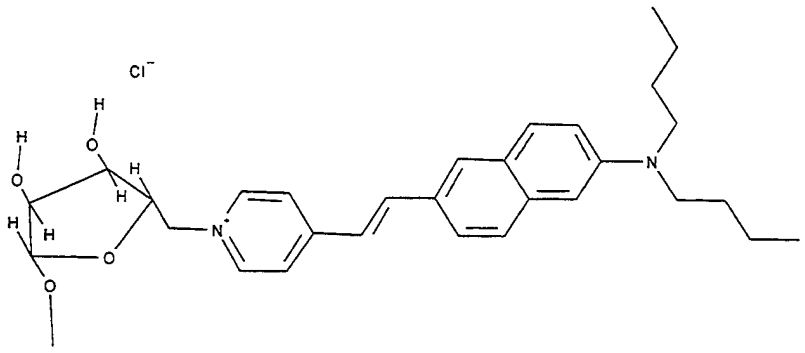

JPW1259

These expectations were realized with several new compounds, but most notably by the dye JPW1259 which has a chiral ribose moiety appended to the pyridinium nitrogen. The second harmonic signal displayed by these dyes is indeed sensitive to membrane potential. The voltage-dependent modulation of the second harmonic signal from a model lipid bilayer membrane stained with JPW1259 was demonstrated by Bouevitch et al.[20] The amplitude of the modulation is linearly dependent on the membrane potential.

In unpublished work with the laboratory of A. Lewis, we have shown that physiological responses from living cells can be monitored with this technique. The experiment involved focusing the 1064 nm light from a q-switched mode-locked Nd-YAG laser onto the visual receptor cells of the house fly. By focusing the light through a microscope and using the high power picosecond pulses available with this laser, it was possible to detect SHG from the JPW1259-stained cells. The SHG signal was modulated by excitation of the receptor with visible light. Clearly such an experiment could not be achieved with linear optical probe excitation because the visible light would itself stimulate the receptor cells. The physiological responses of the preparation match those known from microelectrode studies but, of course, have the advantage of being relatively non-invasive and permitting simultaneous spatial and temporal mapping of activity.

4. MEMBRANE POTENTIAL OF SINGLE CELLS AND ORGANELLES WITH NERNSTIAN REDISTRIBUTION DYES

4.1 Principle of Nernstian redistribution dyes

The idea of redistribution dyes originated in the laboratory of Alan Waggoner.[21-23] This laboratory synthesized positively charged cyanine dyes whose spectral properties have high sensitivities to membrane potential, albeit over slow timescales. The delocalization of the positive charge on these molecules renders them membrane-permeant. Therefore, the equilibrium distribution across the membrane may be governed by the Nernst equation:

$$\Delta V = -60 \log\left(\frac{[dye]_{in}}{[dye]_{out}}\right) mV \qquad (1)$$

Thus, the potential difference across the membrane, ΔV, drives an uneven distribution of dye between the cell interior and the extracellular medium. For the cyanines, the dye distribution generally deviates significantly from that predicted by the Nernst equation because of significant binding to the plasma and organelle membranes and the tendency of these compounds to form aggregates when their concentrations exceed a threshold. Indeed, it is these features of the chemistry of the cyanines which make their spectral properties so sensitive to potential: membrane bound dye displays enhanced fluorescence while dye aggregates have low fluorescence quantum yields. The cyanine dyes can therefore have complex spectral response to potential which depend strongly on the cell:dye ratio, the hydrophobicity of the dye and the particular cell type. Binding to mitochondria and possible responses to mitochondrial potential changes add further complications. Still, with careful calibration protocols, these indicators have been extremely successful for studies of bulk cell populations and remain the best choice for such applications.

This laboratory has aimed to extend the use of permeant cationic dyes to permit quantitative imaging of membrane potential in individual cells.[24-28] The idea was simply to substitute fluorescence intensities for dye concentrations in the Nernst equation to calculate the membrane potential. It became necessary, therefore, to find a dye whose fluorescence intensity both inside and outside the cell is proportional to its concentration. Also the compound had to equilibrate across the membrane reasonably rapidly. Several commercially available delocalized cationic dyes were screened, including additional members of the rhodamine and cyanine class, in an effort to identify suitable "Nernstian" dyes for imaging of membrane potential.[24, 25] While none of these dyes were ideal, the data from these experiments permitted us to design and synthesize a pair of new dyes, TMRM and TMRE, which closely meet the requirements for Nernstian distributions.

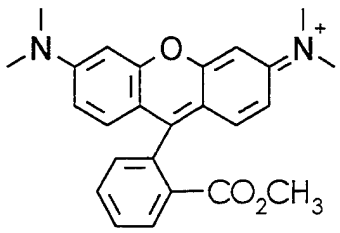

TMRM

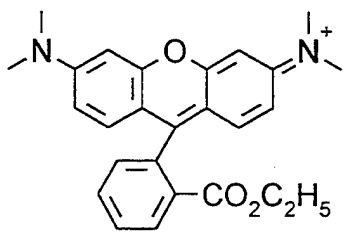

TMRE

4.2 Membrane potential in single cells

These dyes, members of the rhodamine family, are rapidly and reversibly equilibrated across membranes in a voltage-dependent manner governed by the Nernst equation. It was possible to distinguish between changes in mitochondrial and plasma membrane potential with video microscopy[26] but the intensity measurements through a widefield microscope are not strictly proportional to dye concentration. So the Nernst equation cannot be applied directly to intensities to obtain absolute values for the membrane potentials.. The difficulty is that both the fluorescence from the mitochondrion and an adjacent equivalent cytosolic are diluted by volumes sampled by the microscope optics above and below the locations of the cell or its mitochondria.. Confocal microscopy limits the thickness of the volume from which fluorescence is detected. This technique has been used to provide better estimates of the required intensities and can be directly used to measure plasma membrane potential.[29, 30] It is still not suitable for mitochondrial potential (Vmit) because even a confocal optical slice is still too thick to be fully within the volume of typical mitochondria.

4.3 Quantitative 3D imaging permits the measurement of Vmit

To deal with the issue of quantitative intensity measurements from subresolution objects like mitochondria, a calibration scheme must be devised. The approach we chose makes use of the experimental point spread function (psf) of the microscope optics. This is acquired by collecting a high resolution 3D dataset of the fluorescence from a sub-resolution fluorescent bead. This psf therefore can be used to represent how each point in a fluorescent object is blurred by the microscope. In mathematical terms, the convolution of the psf with the 3D distribution of fluorescence density should produce an image identical to that which would be produced by the microscope. A stratagem complementary to confocal microscopy for eliminating out-of-focus contributions in a microscope image involves computer algorithms which use the experimental 3D psf of the microscope to iteratively deconvolve 3D widefield datasets.[31-34] This method effectively takes the out-of-focus fluorescence measured in the experimental data and restores it to its appropriate point of origin..

We have employed such restored images of TMRE fluorescence from the neurites of N1E-115 neuroblastoma cells to determine Vmit of individual mitochondria.[13] The approach involved using restored widefield images and a calibration factor derived from a blurred and then restored model mitochondrion. The key to the construction of this model was the very uniform geometries of the mitochondria in the neurites. Electron microscopy revealed the mitochondria to be a very homogeneous population of cylindrical objects lying parallel to the coverslip substrate and with diameters of 230 nm. The model was taken, therefore as a cylinder of 230 nm diameter, a length of 1000 nm (i.e. well above the xy resolution) and an arbitrarily assigned uniform fluorescence density of 10^4 intensity units. In a typical experiment using a 63X NA1.4 objective, the psf blurred the model to a maximum of only 150 intensity units; restoration brought the intensity back up to 3000 intensity units. Thus the final calibration factor for the intensities in the restored images of the individual mitochondria was taken as 3.3 and accurate membrane potentials could be derived. In recent unpublished studies, we have simplified this approach to work directly with unrestored confocal images and with other cell lines. The calibration factors are higher for confocal images (12 to 16 for the neuroblastoma mitochondria) but the final results are identical.

Using this methodology, several interesting and unique finding were established. The mitochondria have a mean Vmit of -150mV with a significant distribution around the mean of as much as ±11mV (SD). Occasional transient depolarizations of Vmit were observed with magnitudes of 10 to 20 mV. There was no correlation between the motion of individual mitochondria and their membrane potential. The motion stopped well after depolarization of the mitochondria with uncouplers. In a separate study,[35] we tested the response of Vmit to physiological intracellular calcium signals. It was determined that a cytosolic calcium rise, whether by entry through membrane channels or release from internal stores, evoked a ca. 20mV depolarization of the mitochondria.

5. CONCLUSION

This brief overview of 3 new approaches toward membrane potential measurements is designed to demonstrate the power of the confluence of dye chemistry, modern optical technologies, and computational advances in image processing and analysis. It also demonstrates that new secrets are still to be revealed in the ways the cell uses the electrical potentials of its plasma and organelle membranes.

6. ACKNOWLEDGEMENTS

I would like to thank my collaborators at UCHC and in the laboratories of Fred Fay at U. Mass. Medical School and Aaron Lewis at Hadassah Medical School. Also, I would like to acknowledge the financial support of the National Institute of General Medical Sciences and the Office of Naval Research.

7. REFERENCES

1. L. M. Loew, S. Scully, L. Simpson and A. S. Waggoner. "Evidence for a Charge-Shift Electrochromic Mechanism in a Probe of Membrane Potential," Nature, Vol. 281, pp. 497-499, 1979.

2. L. M. Loew, L. Simpson, A. Hassner and V. Alexanian. "An unexpected blue shift caused by differential solvation of a chromophore oriented in a lipid bilayer," J. Am. Chem. Soc., Vol. 101, pp. 5439-5440, 1979.

3. L. M. Loew, G. W. Bonneville and J. Surow. "Charge Shift Optical Probes of Membrane Potential. Theory," Biochemistry, Vol. 17, pp. 4065-4071, 1978.

4. A. Grinvald, L. B. Cohen, S. Lesher and M. B. Boyle. "Simultaneous Optical Monitoring of Activity of Many Neurons," J. Neurophysiol., Vol. 45, pp. 829-840, 1981.

5. J. S. Kauer, D. M. Senseman and L. B. Cohen. "Odor-elicited Activity Monitored Simultaneously from 124 Regions of the Salamander Olfactory Bulb using a Volatage-sensitive Dye," Brain Research, Vol. 418, pp. 255-261, 1987.

6. J.-y Wu, L. B. Cohen and C. X. Falk. "Neuronal activity during different behaviors in aplysia: a distributed organization?," Science, Vol. 263, pp. 820-822, 1994.

7. D. Gross, L. M. Loew and W. W. Webb. "Spatially Resolved Optical Measurement of Membrane Potential," Biophys. J., Vol. 47, p. 270, 1985.

8. R. S. Bedlack, M.-d Wei and L. M. Loew. "Localized membrane depolarizations and localized intracellular calcium influx during electric field-guided neurite growth," Neuron, Vol. 9, pp. 393-403, 1992.

9. R. S. Bedlack, M.-d Wei, S. H. Fox, E. Gross and L. M. Loew. "Distinct electric potentials in soma and neurite membranes," Neuron, Vol. 13, pp. 1187-1193, 1994.

10. P. Shrager and C. T. Rubinstein. "Optical measurement of conduction in single demyelinated axons," J. Gen. Physiol., Vol. 95, pp. 867-890, 1990.

11. S. Antic and D. Zecevic. "Optical signals from neurons with internally applied voltage-sensitive dyes," J. Neurosci., Vol. 15, pp. 1392-1405, 1995.

12. B. M. Salzberg. "Optical Recording of Voltage Changes in Nerve Terminals and in Fine Neuronal Processes," Ann. Rev. Physiol., Vol. 51, pp. 507-526, 1989.

13. L. M. Loew, R. A. Tuft, W. Carrington and F. S. Fay. "Imaging in 5 dimensions: Time dependent membrane potentials in individual mitochondria," Biophys. J., Vol. 65, pp. 2396-2407, 1993.

14. L. M. Loew and L. Simpson. "Charge Shift Probes of Membrane Potential. A Probable Electrochromic Mechanism for ASP Probes on a Hemispherical Lipid Bilayer," Biophys. J., Vol. 34, pp. 353-365, 1981.

15. L. M. Loew. Spectroscopic Membrane Probes, Chapter 14, CRC Press Inc., Boca Raton, Fl., 1988.

16. V. Montana, D. L. Farkas and L. M. Loew. "Dual Wavelength Ratiometric Fluorescence Measurements of Membrane Potential," Biochemistry, Vol. 28, pp. 4536-4539, 1989.

17. C. Zheng and G. Vanderkooi. "Molecular origin of the internal dipole potential in lipid bilayers: calculation of the electrostatic potential," Biophys. J., Vol. 63, pp. 935-941, 1992.

18. J. C. Franklin and D. S. Cafiso. "Internal electrostatic potentials in bilayers: measuring and controlling dipole potentials in lipid vesicles," Biophys. J., Vol. 65, pp. 289-299, 1993.

19. J. Y. Huang, A. Lewis and L. M. Loew. "Non-linear Optical Properties of Potential Sensitive Styryl Dyes," Biophys. J., Vol. 53, pp. 665-670, 1988.

20. O. Bouevitch, A. Lewis, I. Pinevsky, J. P. Wuskell and L. M. Loew. "Probing membrane potential with non-linear optics," Biophys. J., Vol. 65, pp. 672-679, 1993.

21. P. J. Sims, A. S. Waggoner, C.-H. Wang and J. F. Hoffman. "Studies on the Mechanism by Which Cyanine Dyes Measure Membrane Potential in Red Blood Cells and Phosphotidylcholine," Biochemistry, Vol. 13, pp. 3315-3330, 1974.

22. A. S. Waggoner. "Dye Indicators of Membrane Potential," Ann. Rev. Biophys. Bioeng., Vol. 8, pp. 847-868, 1979.

23. A. S. Waggoner. "Dye Probes of Cell, Organelle, and Vesicle Membrane Potentials," The Enzymes of Biological Membranes, A. N. Martonosi, Ed. pp. 313-331, Plenum, New York, 1985.

24. B. Ehrenberg, V. Montana, M.-d Wei, J. P. Wuskell and L. M. Loew. "Membrane Potential can be Determined in Individual Cells from the Nernstian Distribution of Cationic Dyes," Biophys. J., Vol. 53, pp. 785-794, 1988.

25. B. Ehrenberg, M. D. Wei and L. M. Loew. "Nernstian Dye Distribution Reports Membrane Potential in Individual Cells," Membrane Proteins, S. C. Goheen, Ed. pp. 279-294, Bio-Rad Laboratories, Richmond, CA, 1987.

26. D. L. Farkas, M. Wei, P. Febbroriello, J. H. Carson and L. M. Loew. "Simultaneous Imaging of Cell and Mitochondrial Membrane Potential," Biophys. J., Vol. 56, pp. 1053-1069, 1989.

27. D. Gross and L. M. Loew. "Fluorescent Indicators of Membrane Potential: Microspectrofluorometry and Imaging," Methods in Cell Biology, Y. Wang and D. L. Taylor, Ed. Vol. 30, pp. 193-218, Academic Press, New York, 1989.

28. L. M. Loew, D. L. Farkas and M.-d Wei. "Membrane potential imaging: ratios, templates, and quantitative confocal microscopy," Optical Microscopy for Biology, B. Herman and K. Jacobson, Eds. pp. 131-142, Wiley-Liss, New York, 1990.

29. L. M. Loew. "Measuring membrane potential in single cells with confocal microscopy," Cell Biology: A Laboratory Handbook, J. E. Celis, Ed. Vol. 2, pp. 399-403, Academic Press, San Diego, 1994.

30. L. M. Loew. "Confocal Microscopy of Potentiometric Fluorescent Dyes," Cell Biological Applications of Confocal Microscopy. Methods in Cell Biology, B. Matsumoto, Ed. Vol. 38, pp. 194-209, Academic Press, Orlando, 1993.

31. W. Carrington and K. E. Fogarty. "3-D molecular distribution in living cells by deconvolution of optical sections using light microscopy," Proceedings of the 13th annual Northeast Bioengineering Conference, K. Foster, Ed. pp. 108-111, IEEE, 1987.

32. F. S. Fay, W. Carrington and K. E. Fogarty. "Threee-dimensional molecular distribution in single cells analyzed using the digital imaging microscope," J. Microsc., Vol. 153, pp. 133-149, 1989.

33. D. A. Agard. "Optical Sectioning Microscopy: Cellular Architecture in Three Dimensions," Ann. Rev. Biophys. Bioeng., Vol. 13, pp. 191-219, 1984.

34. D. A. Agard, Y. Hiraoka, P. Shaw and J. W. Sedat. "Fluorescence microscopy in three dimensions," Methods in cell biology, D. L. Taylor and Y. Wang, Eds. Vol. 30, pp. 353-377, Academic Press, San Diego, 1989.

35. L. M. Loew, W. Carrington, R. Tuft and F. S. Fay. "Physiological cytosolic Ca2+ transients evoke concurrent mitochondrial depolarizations," Proc. Natl. Acad. Sci. U. S. A., Vol. 91, pp. 12579-12583, 1994.

Biophysical Journal Volume 65 August 1993 672-679

Probing Membrane Potential with Nonlinear Optics

Oleg Bouevitch,* Aaron Lewis,* Ilan Pinevsky,* Joseph P. Wuskell,‡ and Leslie M. Loew‡

*Division of Applied Physics, Hebrew University of Jerusalem and Hadassah Hospital Laser Center, Jerusalem, Israel; ‡Department of Physiology, University of Connecticut Health Center, Farmington, Connecticut 06030 USA

ABSTRACT The nonlinear optical phenomenon of second harmonic generation is shown to have intrinsic sensitivity to the voltage across a biological membrane. Our results demonstrate that this second order nonlinear optical process can be used to monitor membrane voltage with excellent signal to noise and other crucial advantages. These advantages suggest extensive use of this novel approach as an important new tool in elucidating membrane potential changes in biological systems. For this first demonstration of the effect we use a chiral styryl dye which exhibits gigantic second harmonic signals. Possible mechanisms of the voltage dependence of the second harmonic signal are discussed.

INTRODUCTION

Nonlinear optics is an area of considerable current interest. Nonlinear optical phenomena are formally described by the optically induced polarization density, P, which characterizes the optical response of materials to electromagnetic radiation. P can be expanded as a power series in the electric field. The second order term in this expansion, which is composed of the square of the incident electric field and the second order susceptibility, governs the best understood of those optical processes that are nonlinear in the electric field. This second order term is responsible for such nonlinear effects as second harmonic generation, sum and difference frequency generation, the rectification of light and the electrooptic (Pockells) effect.

There have been relatively few direct applications of such second order processes to understanding the structure and function of biological systems. The only investigations to date have used second harmonic generation (SHG). One set of these investigations used the characteristics of SHG and second harmonic microscopy from rat tail tendon to understand details of the structure of this biological system (1, 2). Another set of such studies was aimed at both structural (3) and functional (4) questions that were related to the nature of light-induced proton pumping in the membrane protein bacteriorhodopsin. In this paper we demonstrate that SHG can be used as a monitor of membrane potential and this could be of considerable significance as a new tool in the arsenal of biophysicists interested in investigating the electrical processes that govern biological function.

Optical techniques for monitoring membrane potential were introduced 20 years ago by L. B. Cohen and his colleagues (5) and are now used in a wide variety of research problems (6). Presently, the most popular optical mode for monitoring membrane potential is fluorescence. In this linear spectroscopic approach the fluorescence intensity is monitored as a function of membrane potential. It has been shown that the fluorescence intensity of a dye can be altered by membrane potential primarily in one of three ways: first, by a reorientational mechanism in which a membrane-bound dye tilts in response to an electric field (7); second, by a voltage-dependent redistribution mechanism in which the fluorescent dye partitions into the membrane as a function of the electrical potential (8); and third, by an electrochromic mechanism in which the electric field directly perturbs a dye's electronic transition (9, 22). Such an optical methodology has been found to be very useful in answering a variety of biological questions which require parallel detection of membrane potential over a defined area with relatively high spatial resolution.

In view of the availability of an optical methodology for monitoring alterations in the potential of a membrane, what is the importance for biology of probing membrane potentials with SHG? First, it should be noted that the fundamental laser beam that is used to elicit the SHG can be in the infrared and the infrared nature of the light source should be specifically significant in preventing damage to photosensitive biological systems and to the fluorescent voltage-sensitive probe which readily bleaches as a result of the visible illuminating light source. In addition, unlike the case of fluorescence, in SHG the molecules endocytotically internalized into the cell will not contribute to the observed signal. This results from the fact that symmetry considerations forbid second harmonic generation in an isotropic medium in the electric dipole approximation. Therefore, only those asymmetrically distributed molecules in the membrane will be responsible for the signal without any of the background normally seen when fluorescence is used as the probe. Moreover, because the second harmonic signal is generated instantaneously the only limitation to the kinetic detection of membrane potential with this technique, besides the signal-to-noise considerations to be discussed below, is in the time response of the dye and that is very fast (less than femtoseconds) for the electrochromic molecules that we have chosen for the measurements reported in this paper. Furthermore, in terms of microscopy, second harmonic microscopy will allow the interrogation of

Received for publication 22 January 1993 and in final form 10 May 1993.

Address reprint requests to Aaron Lewis.

0006-3495/93/08/672/08 $2.00

thick tissue slices, such as networks of neurons in brain slices, that can be monitored with the added three-dimensional spatial resolution normally associated with nonlinear optical processes (10). Of special importance in this regard is the dramatic reduction in scattering that occurs with the infrared light that is used to elicit the second harmonic signal. Finally, it should be noted that surface enhancement phenomena that have been used very effectively in such linear processes as Raman scattering have only a marginal effect on fluorescent signals. In terms of nonlinear optical phenomena however, these enhancement factors can occur, and, the enhancements observed for nonlinear processes are at least four orders of magnitude greater than those observed in Raman scattering (11). Thus, one can conceive of an experiment in which a nanometer-sized silver particle, that is chemically directed to a specific subset of membrane proteins, can be used to enhance selectively the SHG of dye molecules in close proximity to this subset of proteins. Such an approach, together with our demonstration of the membrane potential sensitivity of SHG, holds promise of eventually developing an optical, noncontact, analog to the extremely successful method of patch clamping for measuring the electrical properties of membranes around specific protein channels. Therefore, for all of these reasons the study of alterations in the surface SHG as a function of changes in cell membrane potential should be most interesting.

In this paper we present the first steps in this new approach to membrane potential measurements. For this demonstration of the inherent sensitivity of SHG to membrane potential we chose dye molecules that undergo internal charge transfer and can bind and orient in a lipid bilayer. Such molecules fall in the category of dyes that respond to membrane potential by an electrochromic mechanism (9, 22) and large second harmonic signals that have already been detected for monolayers of these compounds (12). In this work, a chiral group is covalently incorporated into the structure since this helps assure a noncentrosymmetric environment for the dye molecules (13). Indeed, our investigations establish an enhancement in the second harmonic signal upon introduction of a chiral center. Furthermore, we demonstrate for the first time the sensitivity of SHG to membrane potential using a hemispherical lipid bilayer stained with a potentiometric dye.

MATERIALS AND METHODS

All the experiments were performed on dyes that were inserted at a concentration of approximately 1% in a hemispherical bilayer membrane of oxidized cholesterol. The hemispherical bilayer is a bubble of approximately 3-mm diameter with walls consisting of a bilayer membrane. The bubble, which is filled with a 0.1 M KCl solution in which there is between 0.3–0.5% ethanol, sits at the tip of a Teflon pipette. It is inserted into a 1- × 1-cm glass cuvette that is filled with the same solution as is in the bubble. The detailed procedure of forming such hemispherical bilayers is described elsewhere (14). This model membrane system has been frequently used to characterize the potentiometric responses of fluorescent dyes (7, 9, 22).

The dyes/molecular voltage-sensitive probes used in these experiments (Fig. 1) were synthesized by procedures adapted from Hassner et al. (1984) (15) and added to the 0.1 M KCl bathing solution from 1 mM stock solutions in ethanol.

For the measurements (see Fig. 2) a Coherent Antares Q-switched modelocked Nd:YAG laser was used at a repetition rate of 400 Hz. The laser

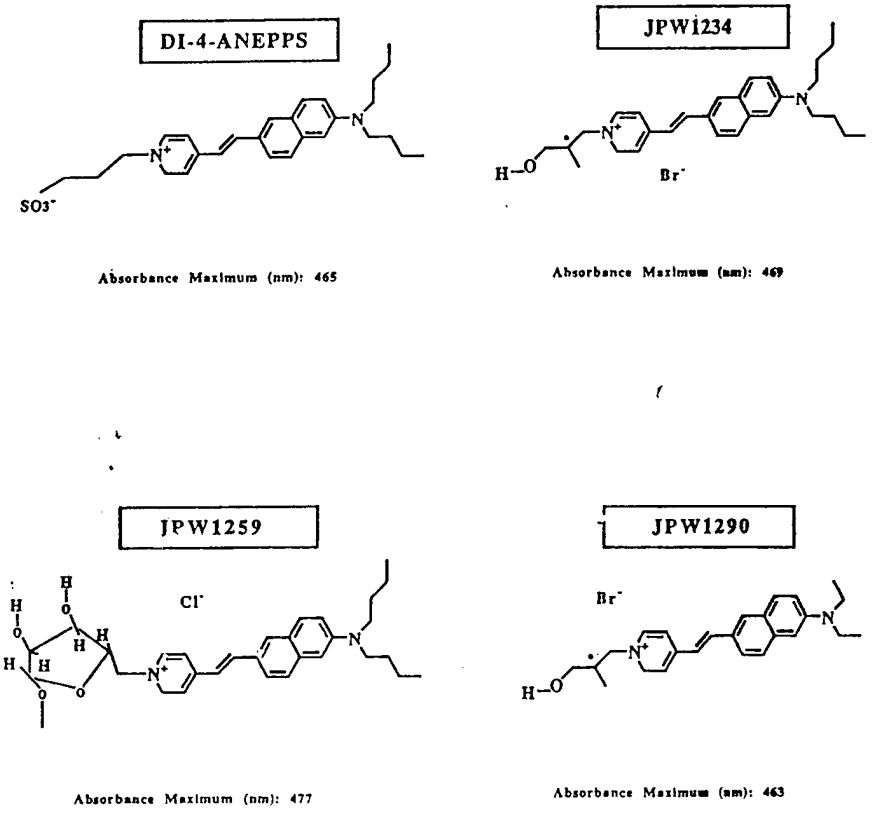

FIGURE 1 Structures of the chiral dyes used in this study. The structure of di-4-ANEPPS (9, 12) is also included for comparison. The wavelength corresponding to the absorbance maximum of dye associated with lipid vesicle membranes is noted below each structure.

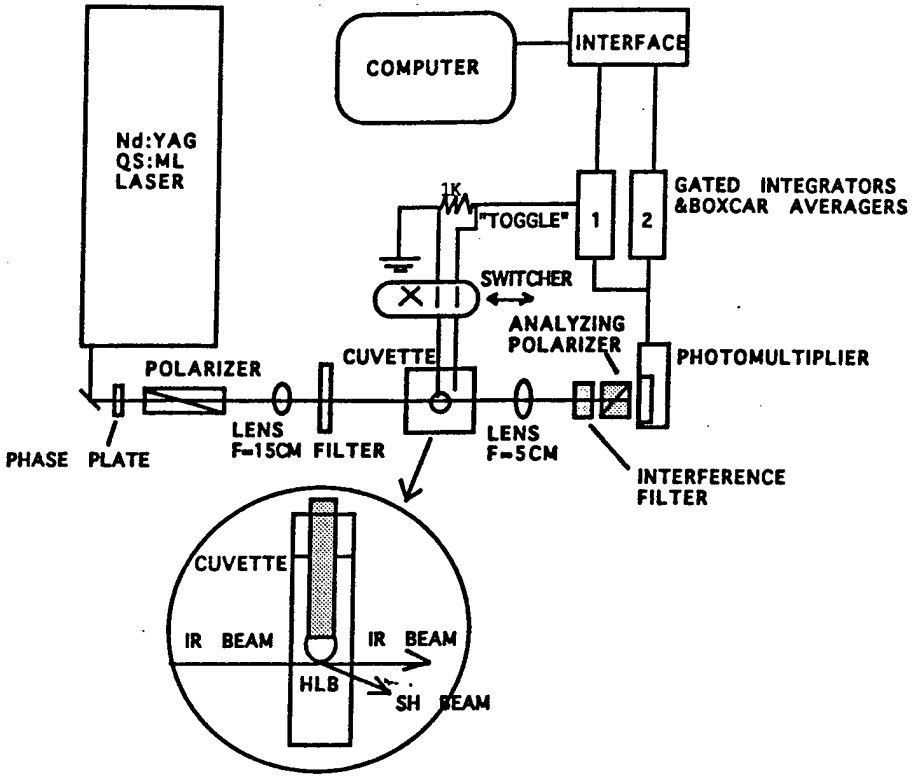

FIGURE 2 A diagrammatic representation of the experimental arrangement used to determine the voltage dependence of the second harmonic response from a dye/molecular probe-labeled HLB.

output was a 300-ns envelope which contained approximately 30 pulses of 120-ps pulse width. The laser pulses were passed through a half-wave plate and a Glan-Thompson laser prism polarizer. The 1064-nm laser power was adjusted to give <100 mW on the sample in a spot size of 180 μm on the bottom of the hemispherical bilayer after the laser had been filtered through a colored glass filter which blocked emissions at wavelengths above 600 nm. The second harmonic signal at a wavelength 532 nm was reflected from the bottom of the bilayer and was passed through an interference filter with a bandwidth of 1 nm followed by a Glan-Taylor prism polarizer. Finally, the signal was directed onto a Hamamatsu R1477 photomultiplier. In some of the preliminary experiments a 30-cm monochromator was used to select the second harmonic wavelength from that of the fundamental. The angle θ of the incident fundamental beam relative to the surface normal was chosen to be ~60° to maximize the second harmonic signal within the constraints of our experimental geometry and in accordance with the expectation that $I(2\omega) \sim \sec^2(\theta)$ (16). The Teflon tip was mounted on a motor-driven X-Y-Z translation stage which allowed the hemispherical bilayer to be freely translated in all three dimensions.

The second harmonic signal and its voltage dependence were detected as shown in Fig. 2 and schematically diagrammed in Fig. 3. The electronics

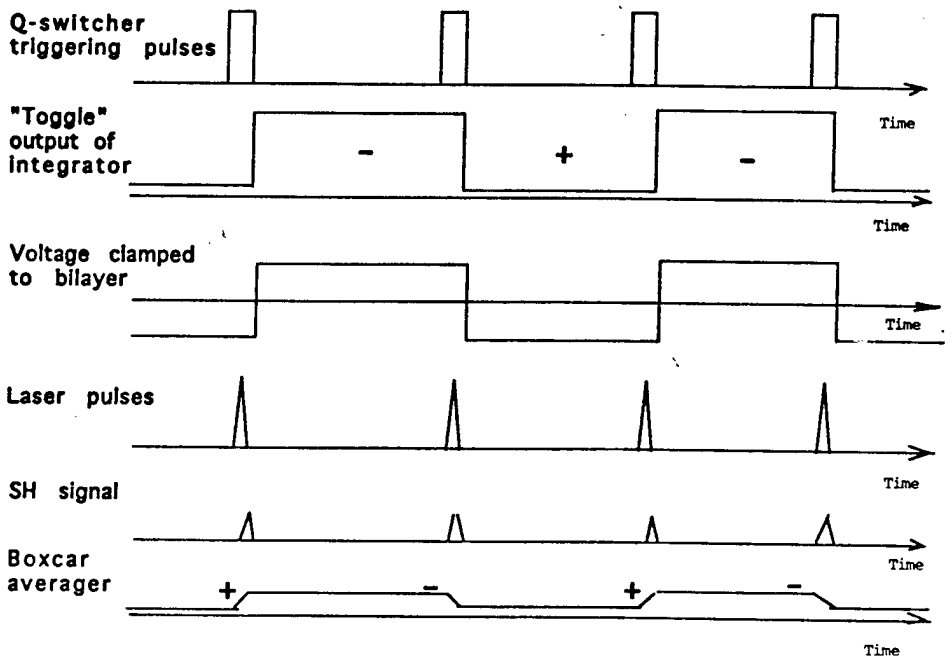

FIGURE 3 A digrammatic illustration of the sequence of steps from laser triggering to boxcar averaging of the signal from the photomultiplier that detects the second harmonic signal corresponding to the membrane potential change.

was synchronized by a triggering pulse from the Q- switcher of the laser as shown in Fig. 3. The photomultiplier output was connected to two Stanford Research (SR250) gated integrators and boxcar averagers. One of these, labeled 1 in Fig. 2, was used in "toggle polarity" mode. In this mode, the integrator reverses the polarity of the input signal after each triggering, adding it to the moving average of the integrator. The "toggle" transistor-transistor logic (TTL) output of the integrator follows this polarity and the TTL output is used to produce bipolar rectangular voltage of ±20 mV which is applied to the hemispherical bilayer. This arrangement allows one to accumulate the difference between the energies of every two successive pulses (generated at membrane potentials of opposite sign) directly in integrator 1. This signal is stored in the internal capacitor of the boxcar. In other words the energy of a pair of pulses changes the charge of this capacitor. Integrator 2 simply measures the overall intensity of the second harmonic signal. Special care was taken so that the coefficients of boxcar amplification for both polarities were identical. In addition, shot-to-shot noise of the laser was reduced to 10–15% by careful adjustment of the laser Q-switcher and mode-locker. Second-order field dependencies, together with long-term instability of the membrane itself, led to noise of 40–50% in the second harmonic signal. Thus, in order to detect a second harmonic modulation due to membrane potential changes that are of the order of several percent of the total second harmonic intensity, at least 3000–5000 shots per measurement were accumulated. Furthermore, the dynamic range of the analog amplifiers used in the boxcar is big enough to follow the small changes expected in the signal. In our experiments, we were able to measure 3% modulation in second harmonic signal with an accuracy that was better than 50% of this modulation. To suppress zero drifts in the registering electronics and those caused by instability in the hemispherical bilayer voltage clamping electrodes were switched several times during the experiment. Every time the electrodes were switched the signal representing the second harmonic modulation [$dI(2\omega)$] increased/decreased by approximately the same value thereby giving us confidence that we indeed were observing the optical response to membrane potential modulation. Both signals representing the second harmonic response [$dI(2\omega)$] and second harmonic amplitude [$I(2\omega)$] were digitized and stored in an IBM PC computer. Relative second harmonic response was obtained by dividing the change in $dI(2\omega)$, due to the electrode switching, by $I(2\omega)$.

RESULTS

Previous experimental results had demonstrated that the potential sensitive dyes di-n-ANEPPS or di-n-ASPPS exhibit SHG with high efficiency when oriented in monolayer films (12). The results presented in this paper extend these results in two directions. First, we have prepared hemispherical lipid bilayers (HLB) stained with these dyes at a concentration of 1% as indicated above. With this dye-to-lipid ratio and based on the previous results obtained on these molecules we estimated a surface susceptibility of 2×10^{-16} esu. For such a surface susceptibility we should get approximately 40 photons/Q-switched pulse of our laser which emits 260 MW/cm^2 peak intensity at the fundamental emission of the laser at 1.06 μm. At first glance such a value seems rather small, however, at a repetition rate of 400 Hz, 16,000 photons accumulate in only 1 s and this should be readily detectable even with an ordinary noncooled photomultiplier using the technique described above which is based on gated integration and boxcar averaging. In spite of the fact that such a signal should be detectable in terms of detector sensitivities it could be easily overwhelmed, in our experimental arrangement, by the presence of the reflection of the fundamental of the laser. In fact, the infrared (IR) beam of the laser is not reflected by the tip of the hemispherical bilayer which was the region illuminated and, moreover, the second harmonic

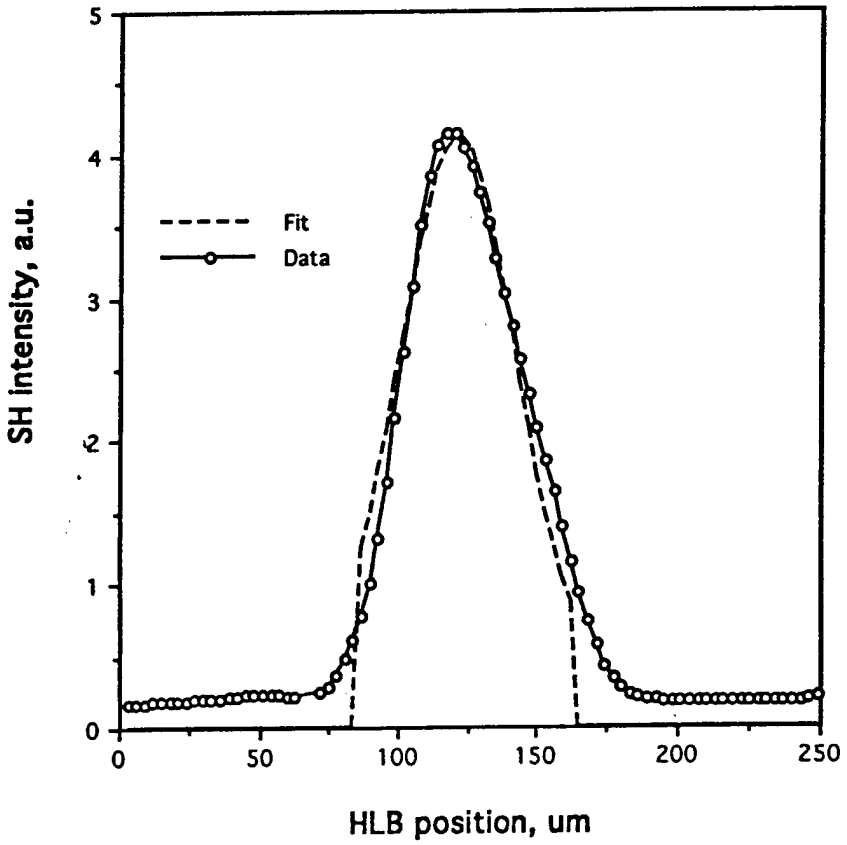

FIGURE 4 The result of slow (10 μm/s) vertical translation at constant velocity of HLB through the IR laser beam focused to 180 μm. The laser worked in a TEM$_\infty$ mode which has a Gaussian lateral intensity distribution. During the translation, the HLB bottom "probes" areas at different local intensity of the IR beam which leads to a corresponding change in the SH signal which is recorded as a function of time. Since the translation is at constant velocity, the form of the curve thereby obtained is close to Gaussian. This fact is illustrated by the solid curve representing the best Gaussian fit of the experimental data. The slight assymmetry of the peak is thought to be caused by the effects associated with the finite curvature of the HLB and the long-term instability of the probe-labeled HLB. The probe in this experiment was merocyanine 540. This probe was added to the HLB by introducing the dye into the surrounding 0.1 M KCl solution at a concentration of 3 μM. All measurements were performed at room temperature. The laser intensity was equal to 300 W/cm^2; peak intensity of the QS:ML pulse was about 260 MW/cm^2; the illumination area on the builayer was 3×10^{-4} cm^2 at the sample. In this experiment the fundamental beam was *s*-polarized and the SH beam was *p*-polarized.

was generated at an angle that was similar to what would be expected for the reflection angle. Thus, we essentially were able to detect the SHG without the presence of any background from the fundamental frequency of the laser.

The SHG from the tip of the dye stained hemispherical bilayer that was observed at 532 nm was well-defined both in terms of its spectrum and in terms of following the temporal nature of the laser pulse. To initially demonstrate the presence of SHG from the HLB we used the dye merocyanine 540 and slowly translated the HLB at a rate of 10 μm/s across a partially focused fundamental beam (FWHM 0.18 mm), while recording the SHG. Fig. 4 shows a typical result of such an experiment. The solid curve is the product of approximating the data by a Gaussian function which should effectively describe the square of the lateral intensity distribution of the fundamental beam. The relatively good fit that was obtained proves that the second harmonic signal is generated by the probe-labeled bilayer. The fact that the second harmonic signal does not go to zero when the bilayer is out of the beam probably results from dye molecules adsorbed to the walls of the cuvette in which the HLB was generated.

We tried to determine the threshold of the fundamental laser intensity at which the second harmonic signal of merocyanine is degraded. This occurred at an intensity of 1 GW/cm^2. At this intensity we succeeded to see an exponential decrease in the signal which is probably due to destruction of the dye molecules by laser heating since the voltage across the bilayer was still detected. In spite of these results we were unable to see any degradation of the second harmonic signal at such intensities when we used the chiral dyes shown in Fig. 1.

With the confidence we developed in seeing the SHG from an HLB we proceeded to monitor this SHG signal as described above. A typical result is seen in Fig. 5 for the dye JPW1259. The absolute second harmonic signal as recorded in integrator 2 is seen in the top of this figure. In the bottom of this figure are the results obtained from reversing the phase of the bipolar voltage across the bilayer. The points at which the phase was reversed are marked with an asterisk. The measurements of SHG were performed with either *s*- or *p*-polarized laser light. The *p*-polarized second harmonic signal was at least one order of magnitude stronger than the *s*-polarized signal, and this was independent of the laser polarization. This means that the probe-labeled bilayer possesses reflection symmetry about any plane perpendicular to the plane of bilayer. Under such symmetry conditions, the only nonvanishing components of the second order surface susceptibility χ are χ_{zxx} and χ_{zzz}. The second order surface susceptibility components of the probe-labeled hemispherical bilayer, χ_{zxx} and χ_{zzz}, and their response to the transmembrane electric field, D_{sp} and D_{pp}, were determined from the measured second harmonic intensities, respectively I_{sp} and I_{pp}, which are proportional to the square of the modulus of the corresponding susceptibilities. (The values D_{sp} and D_{pp} are simply the relative changes in SH signal caused by membrane potential modulation.)

Table 1 provides coparative data for the three chiral dyes, JPW1234, JPW1259, and JPW1290. For the dyes JPW1234 and JPW1259, the value $|\chi_{zxx}|^2/|\chi_{zzz}|^2$ is also given.

DISCUSSION

The molecules synthesized for these measurements have been designed with appropriate donor and acceptor groups and engineered to bind to and orient within a lipid bilayer in order to exhibit a direct electronic response to alterations in

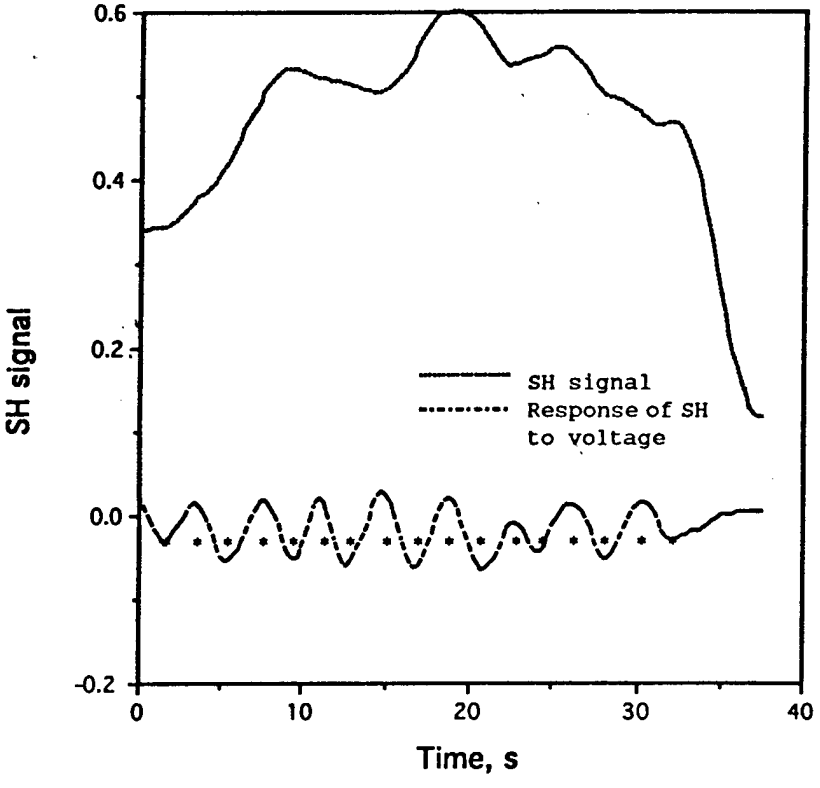

FIGURE 5 Determination of the second harmonic generation dependence on membrane potential. In this experiment, bipolar voltage pulses of ±20mV are clamped to the probe-bound HLB. The QS:ML laser pulses are synchronized with voltage pulses in such a way that QS laser pulse illuminates HLB bottom when positive or negative potential difference on the charging membrane reaches its maximum. Both second harmonic signal (*upper curve*) and its response to modulation of HLB potential (*lower curve*) are recorded simultaneously. To eliminate zero drift in the second harmonic response channel, voltage clamping electrodes are periodically switched. Moments of switching are shown in the figure by asterisks. The probe was JPW1259; bathing solution was 0.1 M KCl in water; concentration of the probe in sultion is 3 μM. All measurements were performed at room temperature. Fundamental intensity was equal to 300 W/cm^2; peak intensity of QS:ML pulse was about 260 MW/cm^2; the illumination area on the bilayer was 3×10^{-4} cm^2 at the sample. In this experiment the fundamental beam was *s*-polarized and the SH beam was *p*-polarized.

Table 1

Dye	D_{sp}	D_{pp}	$\lvert\chi_{zxx}\rvert^2/\lvert\chi_{zzz}\rvert^2$
JPW1234	2.2 ± 0.8	2.2 ± 0.8	1.0 ± 0.5
JPW1259	3.7 ± 0.8	2.8 ± 0.9	1.2 ± 0.5
JPW1290	3.2 ± 1.0	2.2 ± 0.9	

membrane potential. As a result of this design, a change in the wavelength of the absorption maximum of such molecules is detected as a function of membrane potential, and this translates into changes in the fluorescence intensity, which is the method that is presently used with such molecules to detect membrane voltage (9, 22). However, because the presence of strong donor and acceptor groups in these molecules can perturb π electron systems and result in large alterations in the molecular dipole in the vertically excited state, it is well known that these molecular species generally exhibit large nonlinear responses. Therefore, it seemed likely that the very same molecules, that have been shown to be effective in monitoring membrane potential using fluorescence methods, would also be large generators of second harmonic light. To additionally enhance SHG efficiency, chiral groups were incorporated into the polar head regions of the molecules. Furthermore, since the intensity of the second harmonic signal is related to the induced dipole, it was a likely possibility that this signal would be inherently sensitive to membrane potential.

In fact it is important to realize that a wide range of results have been obtained on the potentiometric responses of a variety of molecular probes (7–9, 17, 22), and these results indicate that the second harmonic signal dependence on membrane potential can be caused by one of several factors. These include the orientational response of the dye to membrane potential (7) which would be similar to the well known effect of electric field-induced second harmonic generation or EFISH (18), the possible redistribution of dye molecules with the electric field between different chemical environments such as the lipid membrane and the surrounding solution (8) and the direct electronic response of the dye which is described by the cubic polarizability $\gamma_{ijkl}(-2\omega, \omega, \omega, 0)$ (18). These factors can be expressed as shown below to give the χ(eff), the effective surface susceptibility that is observed.

$$\chi(\text{eff}) = \chi(\text{or}) + \chi(\text{env}) + \chi(\text{e}) \tag{1}$$

There is little doubt that, for different dyes and for various surroundings, the relative contribution of the terms in Eq. 1 will be different. For example, the first term in Eq. 1 is big for dyes which are known to rotate well in the membrane. Thus, if we had used merocyanine 540 in the experiments that measured alterations in the second harmonic signal with membrane potential, then this term would have a major contribution (7). Alternately, Nerstian dyes that partition into the membrane with alterations in membrane potential (8) would be expected to have a dominant contribution from the second term in Eq. 1. Finally, the charge shift probes (9, 22), like the ones that were used in detecting the alterations in the second harmonic signal with membrane potential, are interesting due to the anticipated direct electronic effect on the second harmonic response to membrane potential which should be exhibited universally in various environments (19). As noted above, these dyes are thought to undergo a large induced dipole after interacting with a photon. If the induced dipole is altered by the presence of membrane potential, then this alteration is directly correlated with the molecular hyperpolarizability on which the surface susceptibility and finally the second harmonic signal depends. Thus, one explanation for our observations of the voltage sensitivity of this class of molecules that we have investigated is a direct effect of the membrane potential on the magnitude of the induced dipole.

In support of the dominant contribution in our results of the last term in Eq. 1 is the fact that there is no evidence that such dyes undergo a voltage-dependent partitioning in the membrane and in addition, are not likely to change their orientation in the membrane with membrane potential. The lack of change in orientation is the result of the excellent binding of these molecules in the membrane due to the hydrophobic side chains covalently linked to the aniline nitrogen. The lateral diffusion coefficient of these dyes is equal to 10^{-8} cm^2/s (unpublished results), and this is much less than the square area of the hemispherical lipid bilayer divided by time interval between two successive QS laser pulses, 10^{-2} cm^2/s. This also indicates that migration of the probe molecules along the membrane is unlikely to contribute to the surface susceptibility alterations with membrane potential. Thus, the only term that can effectively describe such electric field induced alterations in the surface susceptibility is the last term in Eq. 1.

In a formal sense this external electric field dependence can be described by the electric field dependence of the β_{zzz} component of the second-order polarizability tensor. Using a nonresonant two-level model (20) β_{zzz} can be expressed as

$$\beta_{zzz} = \frac{3e^2\hbar^2}{2m_e} \frac{W}{[W^2 - (2\hbar\omega)^2][W^2 - (\hbar\omega)^2]} f d\mu_{ex}. \tag{2}$$

Here W is the energy of transition, $\hbar\omega$ is the fundamental photon energy, f is the oscillator strength, and $d\mu_{ex}$ is the difference between the dipole moments in the ground and excited electronic states. The voltage-dependent alterations in $d\mu_{ex}$ probably result in a formal sense from the fact that the linear molecular polarizability in the excited state, P_{ex}, is as a rule bigger than in ground state, P_{gr}, for molecules with long conjugated π-electron systems (21). Thus we can write

$$\beta_{zzz} = \frac{3e^2\hbar^2}{2m_e} \frac{W}{[W^2 - (2\hbar\omega)^2][W^2 - (\hbar\omega)^2]} \cdot f\,[d\mu_{ex0} + (P_{ex} - P_{gr})E]. \tag{3}$$

As a result we get a linear response of the second order polarizability to the electric field E. In this regard it is important to mention that the energy of the electronic transition W also depends on the external electric field due to electrochromism of a molecule (the Stark effect). It is in fact this

dependence which produces the electric field dependence of the optical response of these probes in conventional absorption/fluorescence measurement schemes. Furthermore, when either the fundamental or second harmonic photon energy is close to the electronic transition energy W, the electrochromic effect should be taken into account and Eq. 3 should be accordingly modified to account for damping (21). In our case however, the JPW membrane-bound dye absorption band is centered around 460 nm which is relatively far from second-harmonic resonance in our case (532 nm) and thus this effect should not be contributing significantly. In addition a reorientational mechanism is precluded by the data presented in Table 1 since both D_{sp} and D_{pp} have the same sign which would not take place if reorientation of these probes is taking place in the electric field. If reorientation of the dipole moment of the molecule was occurring it would lead to a response of opposite sign for these different polarization conditions. Thus all our data support a purely electronic effect as a major contributing factor of the electric field dependence of the surface susceptibility.

The probe molecules bind to the outer side of HLB by their hydrocarbon chain which favors orientation of the pyridinium ring near the aqueous interface. Calculations (22) predict that in the excited electronic state the positive charge of the molecule is shifted from the pyridinium end toward the hydrocarbon chain. In our case that means the shift of charge is occurring toward the center of the HLB. Since P_{ex} of a molecule is expected to be bigger than P_{gr}, a positive potential inside the HLB is expected to decrease the induced dipole moment, in accordance with Eq. 3. This leads to decreasing the second harmonic generation efficiency which we indeed have observed experimentally. It is striking that in the case of JPW1259 and JPW1290 dyes the value D_{sp} seems to be bigger than D_{pp}. This is presently not understood.

An important aspect of these studies is to arrive at an estimate of whether real-time measurements of living cell membrane potentials could be made with the unique aspects of second harmonic detection of membrane potential. In such living cellular systems the time response that would be required would be below 1 ms. Since the time response of the second harmonic signal in a purely electronic mechanism is very fast, $<10^{-15}$ s, the essential question is whether there is sufficient signal to noise to allow us to detect alterations in <1 ms. For this estimation, assume that the SHG measurement with a standard deviation 1% allows one to monitor the potential with sufficient accuracy. Based on this assumption and the results of this study, we believe that the best laser system for such measurements would be a cw mode-locked near IR laser source (e.g., a titanium sapphire system) working at a rate of 80–100 MHz. Such a laser system provides 1–5% pulse-to-pulse stability which is necessary for the 1% second harmonic detection accuracy we have assumed. Furthermore, the above-mentioned accuracy requires at least 10^4 photons/1 ms, or a 10^7 photons/s signal power. In view of the above the question that remains is whether such a SHG efficiency can be reached. Let us assume that we are limited by an average intensity of the fundamental laser light which is equal to 300W/cm^2, which was a typical value in our experiments. Such a near IR mode-locked tunable femtosecond laser system, operating at 300W/cm^2 average intensity at a 100-MHz repetition rate and a 100-fs pulse duration, yields about 30 MW/cm^2 peak intensity of the fundamental which is an order of magnitude less than the typical peak intensities of 260 MW/cm^2 employed in the present experiments. Based on the above estimate, of SHG from a probe-labeled lipid bilayer, only 1 photon at the second harmonic frequency is emitted per 100 fundamental femtosecond laser pulses which already gives a fluence of 10^6 photons/s. Moreover, tuning the fundamental laser to 920-nm wavelength will bring the second harmonic emission into resonance with the electronic transition of these probes which should increase the signal by a factor of 100 (12) and yield up to 10^8 photons/s. Thus, the results obtained clearly indicate that the SHG technique is readily applicable to detecting membrane potentials in living cell membranes if the most appropriate laser system that is readily available today is employed. It should be noted in this regard that, the enhancement factors mentioned in the introduction, that are applicable if surface enhancement with silver particles is employed has not been incorporated into these calculations. With such enhancements the time resolution of the method will be based solely on the pulse width of the laser source employed.

CONCLUSION

In conclusion, we have demonstrated that the electric potential of a lipid membrane can be monitored by surface second harmonic generation. A hemispherical bilayer of oxidized cholesterol stained by styryl dyes with chiral centers was used for this demonstration. A qualitative explanation, based on a two level model and a direct electronic response of the induced dipole of a molecule to an external electric field correlates well with our observations. The results obtained clearly indicate that direct measurements of membrane potentials in living cells are possible with this method and such measurements can be obtained with the required time resolution. The intrinsic sensitivity of the technique which promises excellent signal to noise and other important advantages portend extensive use of this new approach.

We are pleased to acknowledge the support of the Office of Naval Research which permitted the initiation of this line of research. Partial support from the U. S. Public Health Service (GM35063) is also gratefully acknowledged.

REFERENCES

1. Freund, I., M. Deutsch, and A. Sprecher. 1986. Connective tissue polarity. Optical second-harmonic microscopy, crossed-beam summation, and small-angle scattering in rat-tail tendon. *Biophys. J.* 50:693–712.
2. Roth, S., and I. Freund. 1981. Optical second-harmonic scattering in rat-tail tendon. *Biopolymers.* 20:1271–1290.
3. Huang, J., and A. Lewis. 1989. Determination of the absolute orientation of the retinyldiene chromophore in purple membrane by a second-harmonic interference technique. *Biophys. J.* 55:835–842.
4. Huang, J., Z. Chen, and A. Lewis. 1989. Second-harmonic generation in purple membrane-poly(vinyl alcohol) films: probing the dipolar characteristics of the bacteriorhodopsin chromophore in bR_{570} and M_{412}. *J. Phys. Chem.* 93:3314–3320.

5. Cohen, L. B., B. M. Salzberg, H. V. Davilla, W. N. Ross, D. Landowne, A. S. Waggoner, and C. H. Wang. 1974. Changes in axon fluorescence during activity: molecular probes of membrane potential. *J. Membr. Biol.* 19:1–36.
6. Loew, L. M., editor. 1988. Spectroscopic Membrane Probes. CRC Press, Boca Raton, FL. Chaps. 14–21.
7. Dragsten, P. R., and W. W. Webb. 1978. Mechanism of the membrane potential sensitivity of the fluorescent membrane probe merocyanine 540. *Biochemistry.* 17:5228–5240.
8. Sims, P. J., A. S. Waggoner, C.-H. Wang, and J. F. Hoffman. 1974. Studies on the mechanism by which cyanine dyes measure membrane potential in red blood cells and phosphatidylcholine vesicles. *Biochemistry.* 13:3315–3330.
9. Fluhler, E. F., V. G. Burnham, and L. M. Loew. 1985. Spectra, membrane binding, and potentiometric responses of new charge shift probes. *Biochemistry.* 24:5749–5755.
10. Wilson, T., and C. Shepard. 1984. Theory and Practice of Scanning Optical Microscopy. Academic Press, London. Chap. 10, pp. 196–209.
11. Wessel, J. 1985. Surface-enhanced optical microscopy. *J. Opt. Soc. Am. B.* 2:1538–1541.
12. Huang, J. Y., A. Lewis, and L. Loew. 1988. Nonlinear optical properties of potential sensitive styryl dyes. *Biophys. J.* 53:665–670.
13. Zyss, J., J. F. Nicoud, and M. Coquillay. 1984. Chirality and hydrogen bonding in molecular crystals for phase-matched second-harmonic generation: N-(4-nitrophenyl)-(L)-prolinol (NPP). *J. Chem. Phys.* 81: 4160–4167.
14. Tien, H. T. 1974. Bilayer Lipid Membranes. Dekker, New York. 478–480, 483.
15. Hassner, A., Birnbaum, D., and L. M. Loew. 1984. Charge-shift probes of membrane potential. Synthesis. *J. Org. Chem.* 49:2546–2551.
16. Heinz, T. F., C. K. Chen, D. Ricard, and Y. R. Shen. 1982. Spectroscopy of molecular monolayers by resonant second-harmonic generation. *Phys. Rev. Lett.* 48:478–481.
17. Dulcic, A. 1979. Some aspects of optical nonlinearity in a new class of conjugated molecules. *Chem. Phys.* 37:57–61.
18. Cheng, L.-T., W. Tam, S. H. Stevenson, G. R. Meredith, G. Rikken, and S. R. Marder. 1991. Experimental investigations of organic molecular nonlinear optical polarizabilities. 1. Methods and results on benzene and stilbene derivatives. *J. Phys. Chem.* 95:10631–10643.
19. Loew, L. M., S. Scully, L. Simpson, and A. S. Waggoner. 1979. Evidence for a charge-shift electrochromic mechanism in a probe of membrane potential. *Nature (Lond.).* 281:497–499.
20. Frazier, C. C., M. A. Harrey, M. P. Cockerman, H. M. Hand, E. A. Chauchard, and C. H. Lee. 1986. Second-harmonic generation in transition-metal-organic compounds. *J. Phys. Chem.* 90:5703.
21. Shen, Y. R. 1984. The Principles of Nonlinear Optics. John Wiley & Sons, New York. p. 17, Eq. 2.17.
22. Loew, L. M., G. W. Bonneville, G. W., and J. Surow. 1978. Charge-shift optical probes of membrane potential. Theory. *Biochemistry.* 17:4065–4071.

Biophysical Journal Volume 71 September 1996 1616–1620

Infrared Nonlinear Optical Measurements of Membrane Potential in Photoreceptor Cells

Ilan Ben-Oren,*# Gadi Peleg,*# Aaron Lewis,*# Baruch Minke,§ and Leslie Loew¶

*The Division of Applied Physics and the Center for Neural Computation, #the Hadassah Hospital Laser Center, the Department of Ophthalmology, and §the Department of Physiology, the Hebrew University of Jerusalem, Jerusalem, Israel; and ¶the Department of Physiology, the University of Connecticut Medical Center, Farmington, Connecticut USA

ABSTRACT In the past it has not been possible to measure optically the membrane potential of cells and collections of cells that are either naturally photosensitive or that can be activated by photolyzable caged transmitter molecules. This paper reports on a unique application of nonlinear optics that can monitor the potential of cellular membranes with a near-infrared source. Among many other singular advantages, this nonlinear optical approach to measuring membrane potential does not activate light sensitive cells or cell suspensions and cellular networks surrounded with photolyzable molecules. To demonstrate this capability we show that the technique can be applied to living photoreceptor cells that are very sensitive to visible light. These cells are ideal for characterizing such a new technique, not only because of their unmatched sensitivity to light, but also because their electrical responses have been extensively characterized (Minke and Selinger, 1992).

INTRODUCTION

The present standard approach to optically measure membrane potential is based on changes in the absorption or the fluorescence of appropriate potential sensitive dyes. There is an enormous amount of literature in this area (Waggoner and Grinvald, 1977; Loew, 1994), but in all the published work it has been impossible to measure optically the membrane potential of photoexcitable cells or associated cellular neural networks surrounded by photoexcitable excitatory or inhibitory molecules. In this paper we demonstrate that the membrane potential of living photoexcitable biological systems can be measured optically using the nonlinear optical phenomenon of second harmonic generation (SHG).

One photon absorption and fluorescence measurement on which previous optical techniques to measure membrane potential are based would excite the photoactivatable molecules, which can trigger cellular physiology. In addition to this obvious and important disadvantage, these linear, one photon techniques suffer from several other limitations in their applicability for monitoring cellular membrane potentials. These limitations include: 1) the poor sensitivity of the linear absorption and fluorescence of potential sensitive dyes to membrane potential; 2) the background contribution of the nonmembrane bound dye molecules; 3) the high cross-section for bleaching the dyes in normal oxygenated physiological conditions; 4) the damaging photoreactions of some potential sensitive dyes such as merocyanine 540; 5) the highly scattering nature of visible light that prevents penetration into the depths of biological media; and 6) the limitations on microscopic resolution that can be obtained with conventional visible light microscopy without signal limiting confocal techniques.

Many of these problems are overcome in this paper by the application of a nonlinear optical process to monitor membrane potential. Specifically, the second-order nonlinear optical process, second harmonic generation, is very sensitive to membrane potential (Bouevitch et al., 1993). In addition, second-order processes require symmetry breaking surfaces (Shen, 1989), such as cell membranes (Huang et al., 1989), and thus, only dye molecules with a distribution between the two layers of a bilayer membrane that lack a center of inversion will produce the directed signals associated with second harmonic generation. Furthermore, the infrared excitation does not affect photoexcitable molecules in and around cells when their one or two photon absorptions occur out of the wavelength regimes that can be significantly excited by the 1.06-μ wavelength of this laser. Also, this radiation can penetrate deeper into cellular media without causing destructive photodamaging effects. Finally, the use of nonlinear processes in this context results in naturally high resolution in x, y, and z and, as has recently been suggested, this resolution can approach 75 nm for appropriate geometries of excitation and detection (Hell, 1994).

Recently, we have been able to demonstrate that appropriately configured molecules could be inserted into model membranes as sensitive nonlinear optical monitors of membrane potential (Bouevitch at al., 1993). In this paper we extend these model system experiments to investigate the light-induced changes in membrane potential of living photoreceptor cells of the fly. The sensitivity of SHG to the electric field in the area of the probing molecular species can originate, in principle, from several molecular processes that have been shown to occur as a result of changes in membrane potential. These processes include alterations in the orientation of the probing molecular species, the Nernstian partitioning of dye molecules between the membrane

Received for publication 5 September 1995 and in final form 10 May 1996.

Address reprint requests to Dr. Aaron Lewis, Division of Applied Physics, School of Applied Science, Givat Ram Campus, Hebrew University, Jerusalem, 91904 Israel. Tel.: 972-2-6798243; Fax: 972-2-6798074; E-mail: lewisu@vms.huji.ac.il.

0006-3495/96/09/1616/05 $2.00

and its surrounding solution, electrochromic changes in the probing dye molecule due to Stark effects on the energy of the electronic transition of the molecule or electrophoretic internalization of the dye molecules from the membrane. It has been shown (Bouevitch et al., 1993) that by way of an electrochromic charge shift mechanism, the membrane potential affects the second harmonic of the dyes that have been designed for monitoring membrane potential and are used in this work.

Theoretical description

When light strikes a molecule it generates a polarization in the electronic distribution that is expressed in Eq. 1.

$$\mathbf{P} = \chi^{(1)}*\mathbf{E}_1 + \chi^{(2)}*E_1*E_2 + \chi^{(3)}*\mathbf{E}_1*\mathbf{E}_2*\mathbf{E}_3 + \ldots \quad (1)$$

The linear spectroscopic methods are governed by the first order term in this expression namely the electric field from the photon $\mathbf{E}_1$ and $\chi^{(1)}$, which defines the polarizability change in the molecule with this electric field. The intensity of the SHG is principally determined by the second order term, $\chi^{(2)}$ in Eq. 1, which defines the second order correction to the polarizability change, and the two electric fields, $\mathbf{E}_1$* $\mathbf{E}_2$, of the two photons that are summed in SHG. Of principal importance to the experiments described in this paper is the fact that all processes defined by $\chi^{(2)}$ can only arise if the molecular species have a distribution that lacks a center of inversion. The intensity of the SHG that is detected is in principle proportional to the square of the incident laser intensity and the appropriate value of $\chi^{(2)}$ for the molecular species in question.

Calibration of the second harmonic signal with membrane potential

To effectively characterize our results on the visual photoreceptor system we have monitored the sensitivity of the SHG to membrane potential in a hemispherical bilayer (HBL) model membrane system. The HBL system has been described previously (Bouevitch et al., 1993). In this system a cholesterol bubble is formed at the tip of a Teflon pipette and electrodes are introduced across the membrane bilayer of the bubble. Several styryl dyes of the form used in the photoreceptor experiments were investigated.

To characterize that our signal was indeed arising from SHG we performed various tests. These included the square dependence of the SH signal on the intensity of the fundamental beam and the spectral characteristics of the SH emission, the time correlation of the SH signal with the infrared pulse, and the spatial characteristics of the SHG. In Fig. 1 the sensitivity of SH signal in an HBL to the amplitude of the membrane potential is shown for the dye JPW 1290. To eliminate from these results the contributions that are not linearly dependent on the electric field, the amplitude of the change for opposite polarities in the field was monitored.

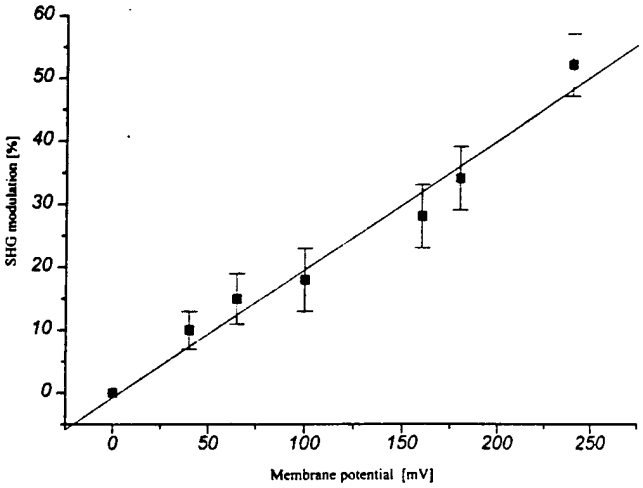

FIGURE 1 The alteration of the second harmonic signal versus the peak to peak amplitude of the modulating voltage with the dye JPW 1290 in a hemispherical bilayer.

The results shown in Fig. 1 clearly indicate the greater sensitivity (as determined from the slope of the linear dependence) of the method with respect to linear optical approaches to membrane potential measurements. In addition to these encouraging results, the data on cellular systems, for example the photoreceptor cells described in this paper or for a variety of cultured cell systems (data not shown), indicate that the sensitivity of the method as monitored in living cells is at least twofold higher from what is reported for the HBL system. In P19 neuronal cell cultures an ~10% change in the SHG with a 10-mV alteration in membrane potential was detected (data not shown). This is five times better than the HBL results reported in Fig. 1 and an order of magnitude better than the best linear fluorescence measurements with the same type of styryl dyes (Gross and Loew, 1984). The HBL result reported in this paper could arise from difficulties in interrogating regions of the HBL system in which the membrane has thinned to a single bilayer.

Experiments with visual photoreceptors and associated neural cells of the fly

The experiments were performed with the experimental arrangement schematically illustrated in Fig. 2. Musca eyes of a white-eyed mutant were partially cut to expose the photoreceptor and/or Lamina neural cells of the living fly, a morphological drawing can be seen in Minke and Selinger (1992). Each of the photoreceptors is connected to the laminar neural cells through an inverting sign synapse.

After staining with the JPW 1259 dye (Bouevitch et al., 1993), the SHG was detected at the reflection angle relative to the incident fundamental laser beam. In addition to the SHG we observed strong two photon fluorescence ~600 nm

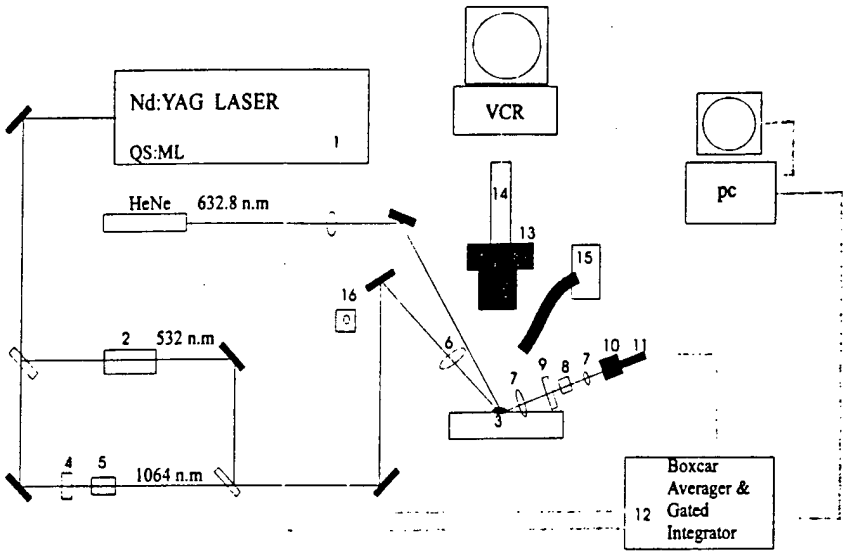

FIGURE 2 A diagrammatic representation of the microscopic second harmonic generation system used in the experiments. Instrumentation: The laser used was a Coherent Radiation Nd:YAG, which was modulated to generate Q-switched, mode-locked (QS:ML) pulses of 1064 nm (1). Each QS:ML pulse is structured from a 300-ns envelope that contains a series of 100-ps pulses. The laser could be doubled to 532 nm for alignment purposes by a Quantum Technology temperature controlled crystal (2), and this laser could be colinearly directed onto the sample (3) with the 1064-nm infrared beam that was appropriately controlled (4, 5, 6) with regard to its intensity, polarization, and spot dimension. The signal was collected from the sample and passed through appropriate lenses (7), polarizers (8), and filters (9) to a monochromator (10) equipped with a Hamamatsu R-1477 photomultiplier tube (11). The signal was recorded and analyzed by a Stanford Research Systems (Sunnyvale, CA), SR240 fast preamplifier, Boxcar Averager and Gated Integrator (12), and a PC. The sample was viewed by a surgical microscope (13) equipped with a charge-coupled-device camera (14) sensitive to the Nd:YAG laser irradiation. The sample could be modulated with light either from a HeNe laser or using a Zeiss (Oberkochen, Germany) fiber illuminator (15) with an orange filter. The infrared intensity was monitored with a fast EG&G Instruments (Princeton, NJ) photodiode (16).

from the labeled preparation. No SHG signals were detected without staining with the dye. We also determined that the visible excitation system used to modulate the photoreceptor physiology did not introduce any signal in the measurement system. In addition, we tested that the modulating visible light did not change the sensitivity of the detection

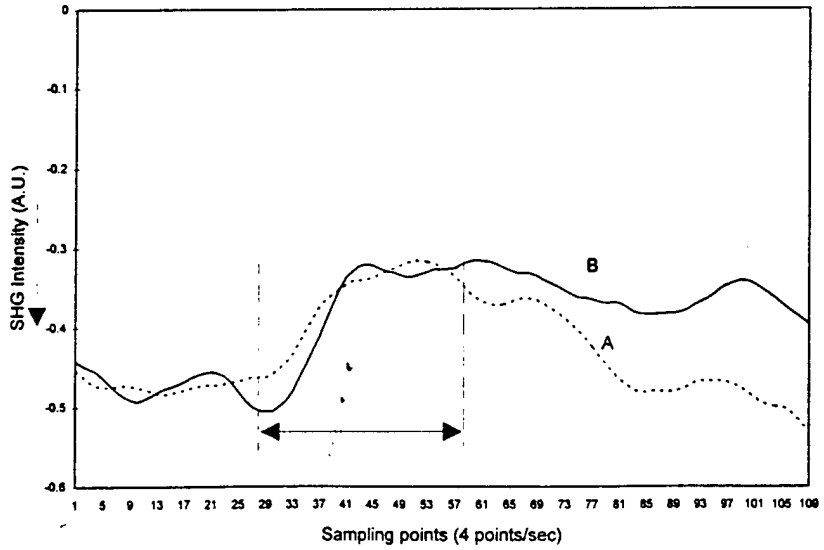

FIGURE 3 (*A*) Second harmonic generation before, during, and after illumination of the sample with orange excitation (*double-headed arrow*). (*B*) The same as *A* except for a sample after repetitive excitation. Methods: White-eyed Musca flies were grown, prepared and cut using standard procedures; the photoreceptor or lamina cells were very sensitive to ethanol in which the potential sensitive second harmonic dyes were dissolved. Thus, the staining of the cells was performed using a filtered Ringer's solution containing the dye JPW 1259. The resulting solution had an optical density of up to 0.3 at 480 nm. To prepare this final solution the dye was first dissolved in 0.25% dimethylsulfoxide, 0.25% ethanol, and 0.05% pluronic F127 (Sigma, St. Louis, MO) for more effective dissolution of the dye. After 5 min in the staining solution, the eyes were washed with the same Ringers solution without the dye present. The SHG signals were averaged using the gated integrator and PC system. This resulted in a response time of ~3 s.

system. The exposed eyes were viewed with a video infrared sensitive microscope to make sure that the fixed eye did not move during the measurement.

The membrane potential of the photoreceptor cells of the fly can be modulated with light. The wavelength of the modulating light is chosen with relation to the relative absorption of the two stable pigment states that are found in this photoreceptor. One of the pigment absorptions corresponds to 490 nm, which is the initial pigment form in the dark, rhodopsin (R_{490}). The other pigment absorption that is of importance to us in this work is the photochemically generated transformed structure of rhodopsin called acid metarhodopsin (M_{570}), which has an absorption at 570 nm. These two pigment forms can be switched optically and as a result a steady-state concentration can be maintained that defines a steady-state membrane voltage that can be monitored. This steady-state voltage is altered by the background level of the light, which causes a relatively rapid light adaptation process. Based on the absorptions noted above, orange light from a fiber optic lamp (<3 mW/cm^2) or a weak beam from HeNe laser (<0.5 mW) can induce steady-state voltage changes across the plasma membrane of the cell. These visible light-induced changes in membrane potential were monitored by the SHG. All experiments were performed in total darkness, except for the controlled exposure of the cells to the visible and infrared light sources mentioned above.

As a result of this visible light excitation of the photoreceptor a depolarization in the membrane potential occurs. This depolarization is seen in Fig. 3 *A*. This figure shows the response of a dark-adapted visual photoreceptor that was exposed to orange light. The light exposure is indicated by the double-headed arrow, which symbolizes the time of the exposure. When the modulating orange light that excited this photoreceptor was turned on, a decrease of ~30% in the signal level was detected. On the other hand, when the modulating light was turned off, a rapid return to the initial signal level is observed.

In Fig. 3 *B* the same procedure was repeated on the same cells after 10 min of repetitive excitations. This protocol resulted in a slower return to the equilibrium physiological voltage as can be seen by the slow return of the SH signal to its initial level. In addition to these results, when the modulation was performed by short sequential exposures to a red HeNe laser beam (see *arrows* 1, 2, and 3 in Fig. 4 *A*), the return to baseline was very rapid but the overall response of the cells was decreased due to desensitization. In contrast to these results, Fig. 4 *B* shows the SH response of the neuronal Lamina cells of a similar preparation as a result of a CW (continuous wave) HeNe laser excitation indicated by the double-headed arrow. As can be seen in this figure a small increase in the SHG level is now seen rather than a decrease as was observed when the fundamental laser beam was directed at the photoreceptor layer. An orange beam generates an undetectable response. The difference in the laminar cell behavior between the red HeNe laser focused excitation and the more diffuse orange excitation is understandable in terms of the known physiology of the system (Minke and Kivschfold, 1980). The laminar cells are connected to several photoreceptors and if the photoreceptors are excited uniformly only transient signals are observed in the laminar cells, whereas when the photoreceptor excita-

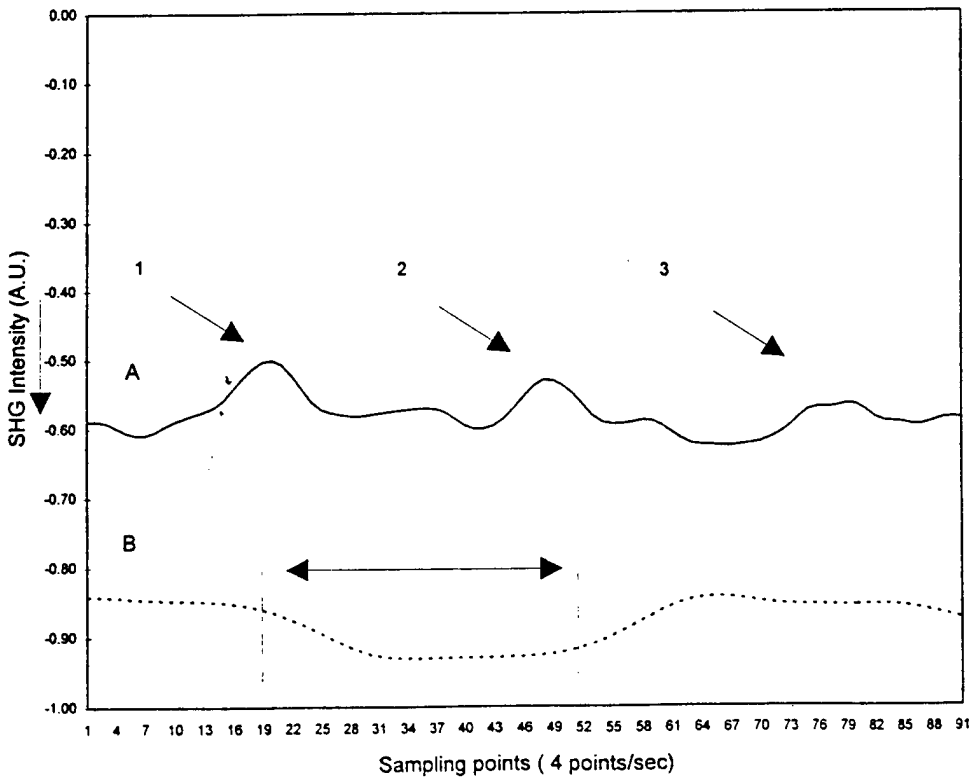

FIGURE 4 (*A*) Second harmonic generation from the photoreceptors cells in the presence of short pulses of excitation (*arrows*) from a HeNe laser. (*B*) The second harmonic generation from neural laminar cells before, during, and after excitation (*double-headed arrow*).

tion is not uniform, as is the case of the HeNe excitation, a direct-current hyperpolarization can be observed.

SHG was very sensitive to membrane potential with changes of at least 30% observed in photoreceptor cells. That such quantitative optical membrane potential measurements can be performed on samples that are highly sensitive to visible excitation is very significant. The photoreceptor cells that we have investigated in this report are archetypical systems of light sensitivity. The fact that such systems, which have extremely well-known physiological properties, can be studied with this optical method of monitoring membrane potential gives us considerable hope that we will be able to extend these measurements to other areas of neuroscience besides the obvious extensions to retinal neural networks.

One such possible extension that is of considerable importance in the field of neuroscience is the optical monitoring of SHG with infrared light in a neural network while a caged excitatory or inhibitory substance is released with visible or ultraviolet light. Not only will such an optical experiment allow for parallel monitoring of a variety of cells, but this can be performed with the excellent imaging capabilities that are inherent in nonlinear optical microscopies, which are experiencing an exponential growth phase in their development at the present time. Finally, it should be noted that the utility of these developments is not limited to problems in neuroscience, but is also of considerable significance in such areas as photosynthesis and other areas of membrane energy transduction. Thus, we believe that monitoring membrane potential with SHG will be a useful new tool not only in neuroscience but in a variety of interesting areas of biology.

We thank the U.S.-Israel Binational Science Foundation and the Office of Naval Research, United States Navy for grants in support of this work. Partial support from the U.S. Public Health Service (GM 35063) is also gratefully acknowledged.

Dr. Boaz Gillo from the Hadassah Hebrew University Medical School is thanked for his assistance.

REFERENCES

Bouevitch, O., A. Lewis, I. Pinevsky, J. P. Wuskell, and L. M. Loew. 1993. Probing membrane potential with nonlinear optics. *Biophys. J.* 65: 672–679.

Gross, D., and L. M. Loew. 1989. Fluorescent indicators of membrane potential. *Methods Cell Biol.* 30:193–218.

Hell, S. W. 1994. Improvement of lateral resolution in far-field fluorescence light microscopy by using two photon excitation with offset beams. *Optic Comm.* 106:19–24.

Huang, J., A. Lewis, and L. M. Loew. 1989. Nonlinear optical properties of potential sensitive styryl dyes. *Biophys. J.* 53:665–670.

Loew, L. M. 1994. Voltage sensitive dyes and imaging neural activity. *Neuroprotocols.* 5:72–79.

Minke B., and K. Kivschfold K. 1980. Fast electrical potentials arising from activation of metarhodopsin in the fly. *J. Gen. Physiol.* 75: 381–402.

Minke, B., and Z. Selinger. 1992. Intracellular messengers in invertebrate-photoreceptors studied in mutant flies. *In* Neuromethods, Vol. 20. Intracellular Messengers. A. Boulton, J. Baker, and C. Taylor, editors. The Humana Press. 517–563.

Shen, Y. R. 1989. Surface properties probed by second-harmonic and sum-frequency genera. *Nature.* 337:519–525.

Waggoner, A. S., and A. Grinvald. 1977. Mechanism of rapid optical changes of potential sensitive dyes. *Ann. N. Y. Acad. Sci.* 303:217–241.

Bioimaging 4 (1996) 215–224. Printed in the UK

Gigantic optical non-linearities from nanoparticle-enhanced molecular probes with potential for selectively imaging the structure and physiology of nanometric regions in cellular systems

Gadi Peleg†, Aaron Lewis†‖, Oleg Bouevitch†, Leslie Loew§, Dorit Parnas‡ and Michal Linial‡

† Division of Applied Physics, Center for Neural Computation and The Hadassah Laser Center, The Hebrew University of Jerusalem, Jerusalem, Israel
‡ The Department of Biological Chemistry, The Hebrew University of Jerusalem, Jerusalem, Israel
§ The Department of Physiology, The University of Connecticut Health Center, Farmington, Connecticut, USA

Submitted 17 July 1996, accepted 17 September 1996

Abstract. The requirement to functionally probe biological structures, with ever increasing selectivity and three-dimensional resolution is a frontier area in microscopy. Non-linear optics has a unique potential in this regard with numerous studies focused on the potential of three-dimensional imaging with super-resolution. In this paper we demonstrate that non-linear optical phenomena, such as second harmonic (SH) generation, which is very sensitive to the membrane potential, can be locally enhanced by complexing or approaching a SH generating molecular probe to a nanoantenna of a silver or gold nanoparticle. This gives complexes with gigantic optical non-linearities. These contrast enhancing non-linear optical complexes have the potential to be directed selectively to specific nanometric regions in cells in order to report on alterations on the structure and the function in such regions while overcoming the inherent inefficiency of non-linear optical interactions.

Keywords: surface enhanced non-linear optical microscopy, nanometric imaging, nanoparticle enhanced probes, second-harmonic generation, two-photon fluorescence, imaging selectivity

1. Introduction

The interaction of light with materials is based on the alterations in the electron density distribution of the material as it co. ples with the interacting photon's electric field, E. These interactions, which characterize the optical response of materials to light, are formally described by a quantity, P, the optically induced polarization density. P can be expanded as a power series in the photon's electric field.

$$P = \chi^{(1)}{*}E + \chi^{(2)}{*}E{*}E + \chi^{(3)}{*}E{*}E{*}E + \ldots .$$

In this expre sion $\chi^{(n)}$ represents the nth-order complex optical susceptibility, which in turn depends on the polarizability tensor which is a quantitative measure of the polarizability of the electron density.

Until recently, practically all imaging applications in biology employed linear optical phenomena that depend on $\chi^{(1)}$. These include such well known processes as

‖ Author to whom correspondence should be addressed. E-mail: lewisu@vms.huji.ac.il

0966-9051/96/030215+10$19.50

the linear absorption and emission of light. In the last few years non-linear optics has begun to make a unique contribution in resolving specific imaging problems in biology that could not be readily addressed with linear spectroscopic techniques. Our efforts have focused on non-linear optical interactions that depend on $\chi^{(2)}$. The specific second order effect that we have focused on is second harmonic generation [1–9]. We have applied this form of non-linear spectroscopy to the understanding of fundamental chromophore protein dipolar interactions [1–5], to answering specific structural questions concerning the absolute orientation of membrane proteins [6] and to developing an exciting new tool for the optical interrogation of cellular physiology, i.e. measuring the membrane potential of cellular membranes [7–9]. Our studies have used the unique feature of second order processes which require the presence of an asymmetric distribution of the second harmonic generators in order to observe the effect. Thus membranes, their proteins and their crucial contribution to cellular physiology are ideally suited to interrogation with such a second order non-linear optical effect.

In addition to our work on the application of non-linear optics to biological systems, there has also been a growing field of activity in the application of a $\chi^{(3)}$ based phenomenon known as two-photon absorption. This activity has been aimed principally at using the spatially limited illumination volume, when pulsed lasers are used to excite non-linear phenomena. Thus, these studies have been aimed at either spatial imaging with a resolution comparable to confocal microscopy but without the need for a confocal aperture [10–13] or spatially confining bleaching [14] and uncaging of cellular activators [15]. The principal differences between two-photon and second harmonic optics arises mainly from the symmetry requirement of second harmonic generation which is not necessary for either third order or first order processes. Thus in second harmonic generation the contribution to the signal of non-relevant inter- and intra-cellular molecules in the surrounding environment is eliminated. The lateral imaging resolution is similar in both techniques, second harmonic and two-photon, and both techniques suffer from a signal that is orders of magnitude weaker than linear optical phenomena.

The object of this paper is mainly to address this last issue of signal to noise in non-linear optical phenomena and therefore to broaden the physiological relevance of these techniques by permitting dynamic effects to be investigated with timescales that are consistent with cellular physiology. As will be apparent, our approach to this problem also has the potential to permit a dramatic increase in spatial resolution with single molecule biological specificity.

An enormous increase in second harmonic generation (SHG), by as much as 2×10^4, was measured for roughened silver surfaces relative to flat silver surfaces [16]. It is generally agreed that this 10^4 signal increase is due to the electromagnetic enhancement of the photon electric field. In addition, Chen *et al* studied the complexation of a monolayer of pyridine to a roughened silver electrode [17]. These investigators found that the presence of pyridine on such a silver electrode increased the 10^4 field enhancement of the roughened silver electrode by as much as 50 times. Such complexation is in analogy to the effect of surface enhancement seen for the linear optical phenomenon of spontaneous Raman spectroscopy on roughened silver surfaces. In this phenomenon, which is known by the acronym of SERS, for surface enhanced Raman spectroscopy, enhancements have been monitored for molecules in close association with roughened silver surfaces of as much as 10^6 but this includes a molecular/chemical component to the interaction which can be a factor of 50. The electromagnetic enhancement arises from a lightning rod phenomenon by which these optical fields are concentrated at the tips of geometric structures and from a plasmon resonance in metals such as silver and gold. The plasmon resonance arises from collective oscillations of the surface electrons in confined nanometric regions.

When cellular imaging is the objective such an approach to enhancing the signal is so limiting geometrically that it has not attracted any interest from the optical imaging community. In this paper, we develop a flexible approach that will allow the enhancement of non-linear optical phenomena to be generally applied to cellular and subcellular spectral imaging with single molecule selectivity and sensitivity. The basis of this approach is to use silver or gold nanoparticles that are either directly complexed to a staining dye or are in close proximity to a stain associated with a specific cellular component. In order to collect enhanced spectroscopic phenomena from nanometric regions of a sample, to demonstrate the feasibility of this approach, we present in this paper a series of non-linear optical investigations on two different dye/nanoparticle systems. One of these systems is a silver colloid aggregate to which is complexed a variety of dye molecules and the other is a cell culture which is stained with a membrane selective SH dye which is in close proximity to silver or gold nanoparticles resting on the cellular membrane. The data we have obtained demonstrate that these silver or gold nanoaggregates, with their highly controlled dimensionality and their well known ability to be selectively directed to single molecules in specific cellular sites as deduced from electron and linear optical microscopy, will make an important contribution to non-linear imaging of cellular structure and physiology. The signal enhancements that can be obtained, even in our present experiments with less than optimal experimental conditions, such as available exciting wavelengths etc, suggest a signal to noise that will allow a variety of non-linear optical imaging modalities to be extended into interesting regimes of resolution and cellular dynamics.

2. Materials and methods

2.1. Dye colloidal aggregates

To produce the dye colloidal aggregates (DCA) the silver colloid [18, 19] was mixed with a CH_2Cl_2 solution of the dye of interest at a concentration of 10^{-4}–10^{-6} M by vigorously shaking the two solutions together for ~ 10 s. Within seconds after mixing, the silver colloid present in the aqueous phase aggregated, probably due to the adsorption of the dye to colloidal particles. In addition, a liquid metal (LM) film appeared at the interface between the organic solvent and water indicating adsorption of dye to the silver colloid [20]. We found that both the interfacial LM film and the DCA aqueous suspension exhibit many similar and very interesting non-linear emission characteristics.

2.2. Silver nanoparticles spread on a thin silver film surface

To investigate the contribution of the silver nanoparticles to the local field enhancement, thin silver films of an approximate thickness of 20 nm were evaporated in a vacuum in order to produce a transparent non-conducting silver film. The silver nanoparticles, described in section 2.3, were deposited on these films. This sample with the Ag microspheres was immersed in the same physiological medium as the cells. The Ag microspheres were spread to the same extent as in the cellular experiments and the sample was irradiated with the same IR laser power as in the cellular experiments. The Ag film was transparent to a degree that allowed the SHG signal from the microspheres to be measured with the same system sensitivity as in the measurements without the film. The bright appearance of the microspheres with the very low background from the film is seen in figure 1.

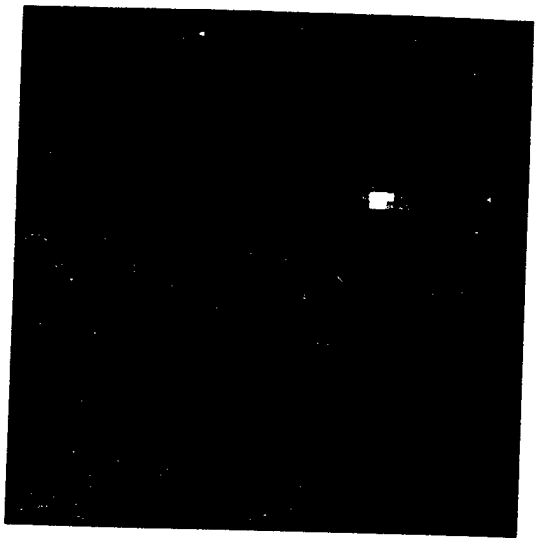

Figure 1. Regions of aggregated silver microspheres on a silver film. Note the very bright appearance of the microspheres and the very low background of the film. The entire field in this image is 25 μm.

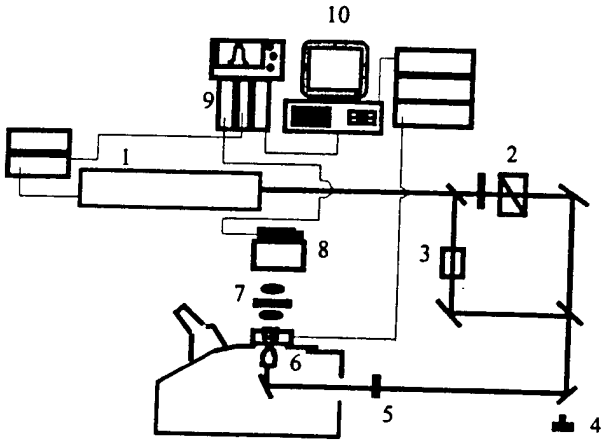

Figure 2. A schematic representation of the experimental arrangement as described in the text.

2.3. Silver and gold colloids associated with cells stained with a second harmonic dye

Undifferentiated P19 neuronal cells and C2 muscle cells were grown on microscope cover slips according to previously published procedures [21, 22] and were maintained in a physiological medium that was composed of 116.1 mM NaCl, 5.4 mM KCl, 2 mM $CaCl_2$, 2 mM $MgCl_2$, 25 mM Hepes, 30 mM glucose, 0.05% BSA at a pH of 7.4. The cells were stained according to the protocol reported earlier [9] and the experiments were performed at room temperature.

The silver and gold microspheres were donated by British Biocell, Cardiff, UK. The particles we used had a diameter of 56 nm for the silver microspheres and 10 and 60 nm for the gold microspheres. Their absorption maxima were at 420 and 550 nm, for the 56 nm Ag and 60 nm Au microspheres respectively. To spread these microspheres on the cell surface 20 μl of a silver or gold microsphere suspension was added to 300 μl of physiological medium in the sample cell positioned on the microscope stage of a special x, y and z scanner. These metal microspheres were deposited by gravitational force onto the cover slip and cells. After 5 min of incubation the coverslip was covered with small continuous islands of Ag microspheres. A few seconds of irradiation with Q-switched mode-locked laser pulses on an island of aggregated Ag microspheres was enough to spread the Ag microspheres from a large island into separate microspheres or very small aggregates.

2.4. The optical system

As seen in figure 2 a Q-switched mode locked Nd:YAG laser (1) with 1.064 μm emission was the illumination source. The average illumination intensity was 1.1 W cm^{-2}

for the dye associated silver colloids and was 400 KW cm^{-2} for the rest of the experiments reported in this paper. The beam was transmitted through a polarizer and a half wave plate for intensity and polarization control (2). Part of this beam was directed through an additional arm (3) in which a non-linear crystal was inserted to produce a green beam to aid in aligning the IR beam. A photodiode (4) was placed in close proximity to the optical path in order to provide a means to monitor the near-infrared (NIR) intensity. A filter (5) was placed in front of the entrance port of the microscope to prevent any second harmonic that was created by the optical elements from entering the microscope. The microscope objectives (6) that were used were either 50 × 0.5 NA or 100 × 1.25 NA. The beam was focused onto the cover slip on which the cells were grown. These cover slips were placed in a special holder into which it was possible to insert a physiological solution.

For some of the experiments the sample was placed on a unique 3-D piezo driven flatscanner from Nanonics, Jerusalem, Israel. This compact scanner which is 7 mm thick and has a central clear aperture can be scanned in x and y with a rough resolution of 1 μm over several millimetres and has fine resolution capability over 30 μm of less than an Ångstrom. It also has the capability of z extensions with the same fine resolution of up to 30 μm.

The non-linear signal was collected with lenses (7) which were held in the condenser track above the sample stage and was detected through a monochromator (8) to measure the wavelength of the effects we observed. The fundamental intensity was blocked by an IR filter. The signal from the photomultiplier was amplified, averaged and integrated by a boxcar averager and a channel integrator (9). These signals were transferred to a computer (10) in which the images were generated. For some of the experiments the detection was accomplished in parallel with a liquid nitrogen cooled charge coupled device (CCD) from Photometrics Inc., Tucson, Arizona.

3. Results and discussion

3.1. Dye colloidal aggregates

The results, presented in this subsection, are split into two parts. The first part (3.1.1) reports on the characteristic linear absorption properties of the LM films, which define the type of resonance effects that can contribute to the intensity of the non-linear measurements. All the evidence presented below indicates that these LM films are colloidal in nature and show all of the enhancement characteristics of the dispersed colloidal aggregates or DCA particles. The second part (3.1.2) of the discussion reports on the non-linear optical phenomena that are observed from both the LM films and aqueous DCA systems.

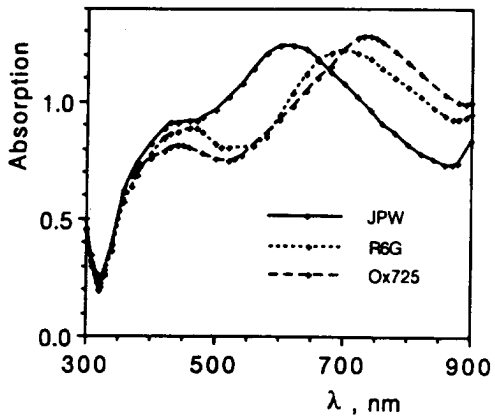

Figure 3. Absorption spectra of liquid metal (LM) monolayers deposited on fused silica. These films complexed from dye molecules have absorptions that are significantly different from the film itself which has a maximum below 400 nm. The dyes are all red-shifted from their absorptions in ethanol which are 528 nm for Rhodamine 6G, 502 nm for JPW 1234 and 643 nm for Oxazine 725 (in Methanol).

3.1.1. Absorption spectroscopy. In order to investigate the enhancement of the absorption properties of the molecular probes by the nanoantennae, we studied the absorption of LM films with UV-VIS-NIR absorption spectroscopy. The absorption spectra of LM monolayers transferred onto a fused silica slide are presented in figure 3.

The LM monolayer films were obtained with the same type of silver colloid and three different types of dyes, JPW1234, Rhodamine 6G, and Oxazine 725. The films were yellow–reddish in color and resembled a vacuum-evaporated gold film. The color shades as observed by the eye were clearly different for the films formed with different dyes. The structure of JPW1234 which is a naphthyl styryl chiral dye with very large non-linear optical effects [7] has been presented previously [8]. The absorption spectra of these dyes vary with solvent but are consistently blue shifted to the absorption of the dye complexed colloids.

A common feature of all three spectra shown in figure 3 is a negative peak at 320 nm. The remaining part of all three spectra consists of two positive peaks in each of the spectra of the three LM films produced with JPW1234, Rhodamine 6G, and Oxazine 725. The first peak in the spectrum occurs at 420, 450, and 440 nm respectively while the second absorption is at 620, 700, and 730 nm.

There are considerable similarities in terms of certain physical properties between the LM (liquid metal) films produced by Gordon *et al* [19] from specific metal complexes and the MELLFs (metal liquid like films) that have been investigated by Efrima and co-workers [20]. These latter MELLFs were produced by stabilizing silver at an aqueous organic interface with a surfactant which had no absorption in the visible region of the spectrum. These workers recorded the absorption spectra of such MELLFs and discovered a negative peak which occurred at 320 nm.

An analogous peak was also observed by Gordon *et al* [19] in their system.

We have also found such a negative absorption peak in our LM films which were prepared by stabilizing silver with a variety of dyes. Efrima and co-workers attributed the negative peak at 320 nm to the colloidal nature of the films they investigated. Thus, our films are colloidal in nature.

In addition to the above, nearly a decade and half ago Garoff *et al* [23] and Craighead and Glass [24] investigated the absorption of silver island films on which dye molecules were deposited. They focused on the modification of the absorption of the silver island film by the dye and found that the plasmon resonance peak of the film was split by the presence of the dye into two peaks. The position of the long wavelength component of these two peaks correlated with the relative visible absorption of the dye. Their results were explained in the framework of Mie theory and this work established that there was a significant degree of electromagnetic interaction between the silver particles and the dye. The results of the electromagnetic calculations indicated that a large fraction of the electromagnetic energy collected by the particle was deposited in the dye [23, 24].

The spectra of our LM films show all of the absorption features mentioned above. They include the splitting of the plasmon resonance peak and the correlation between the absorption maxima of the dye and the position of the long wavelength component. Thus, we can conclude that there exists a strong electromagnetic interaction between the silver colloid and the dye. This interaction leads to a significant deposition of the electromagnetic energy that is received by the silver into the dye molecule.

3.1.2. Emission spectroscopy. There is a strong indication from the results above that the unusual character of non-linear emission observed from the DCA (figure 4), including two- and multiphoton luminescence and SH generation as detailed in the figure caption, is a result of strong electromagnetic interaction between the molecular probe and the nanoantenna of the silver colloid. This conclusion is based on the absorption spectroscopy studies of LM films obtained with the JPW series of dyes (discussed above) which pointed to a significant degree of electromagnetic interaction between the silver particle and the dye coating.

As is seen from figure 4, a pure silver colloid aggregated in an aqueous solution of 0.1M KCl has a SH generation efficiency of the same order of magnitude as a JPW1234-colloid complex. Possibly, the ion-activated interaction between the neighboring silver particles themselves can lead to an efficient SH generation. It is important to mention that the magnitude of SH generation is modulated by the dye used (see figure 4), which is a result of electromagnetic and, probably, chemical interactions between the dye and the silver particle. Since

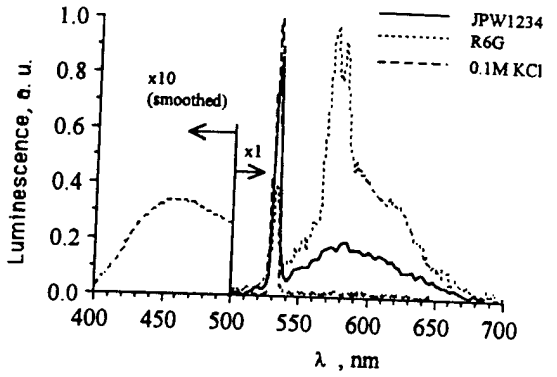

Figure 4. Non-linear emission spectra of an aqueous DCA suspension by a Q-switched mode-locked Nd:YAG laser illumination at 1.064 μm. The average illumination intensity is 1.1 $W\,cm^{-2}$. The figure shows the spectra of DCA particles prepared with JPW1234 and Rhodamine 6G (Rh6G) dispersed in an aqueous solution. In addition a spectrum of silver colloid aggregated in 0.1M KCl is shown. The three wavelength regions relative to the second harmonic wavelength, = 532 nm, > 532 nm and < 532 nm, are associated with different mechanisms of non-linear emission. The region > 532 nm is normally associated with two-photon luminescence. The ratio of the two-photon luminescence which occurs in this region for the different dyes is related to the relative quantum yield of the linear fluorescence: the highly fluorescent dye Rh6G produces a 'luminescent' DCA with a larger two-photon emission than the JPW1234 dye which is normally non-fluorescent when in solution. The origin of the luminescence is not completely understood, especially the two peak structure (peaks occur at 573 and 579 nm) clearly seen for Rh6G particles. The sharp peak at 532 nm is associated with second harmonic (SH), or hyper Raleigh, scattering. The SH efficiency of films/particles formed with JPW1234 dye is higher than the Rh6G particles. This correlates with the high value of the second order polarizability of these styryl dyes [7, 8]. Finally, in the region < 532 nm the luminescence occurs from multiphoton interactions. No multiphoton luminescence from JPW-based particles was detected, whereas the spectrum of Rh6G-based particles clearly exhibits distinguishable multiphoton luminescence at wavelengths of 400–500 nm which, again, correlates with a highly luminescent character of the R6G dye. In order to make evident the presence of multiphoton luminescence, the Rh6G data in the region 400–500 nm in figure 2 are smoothed and multiplied by ten.

the linear/non-linear optical constants of the molecular probe are sensitive to the local parameter being measured [8, 25] the dye colloid aggregates hold promise of being a new kind of efficient non-linear optical nanoprobes. Experiments to test this possibility are under way.

The study of the strength of SH generation as a function of the concentration of the silver in the colloidal suspension and of the dye in the methylene chloride solution before the mixing of the colloid and dye solutions revealed that there is an approximately direct proportionality between the silver concentration used and the optimal concentration of the JPW1234 dye, the optimal ratio being 6μM of the dye per 100 μM of silver. This optimal ratio can be attributed

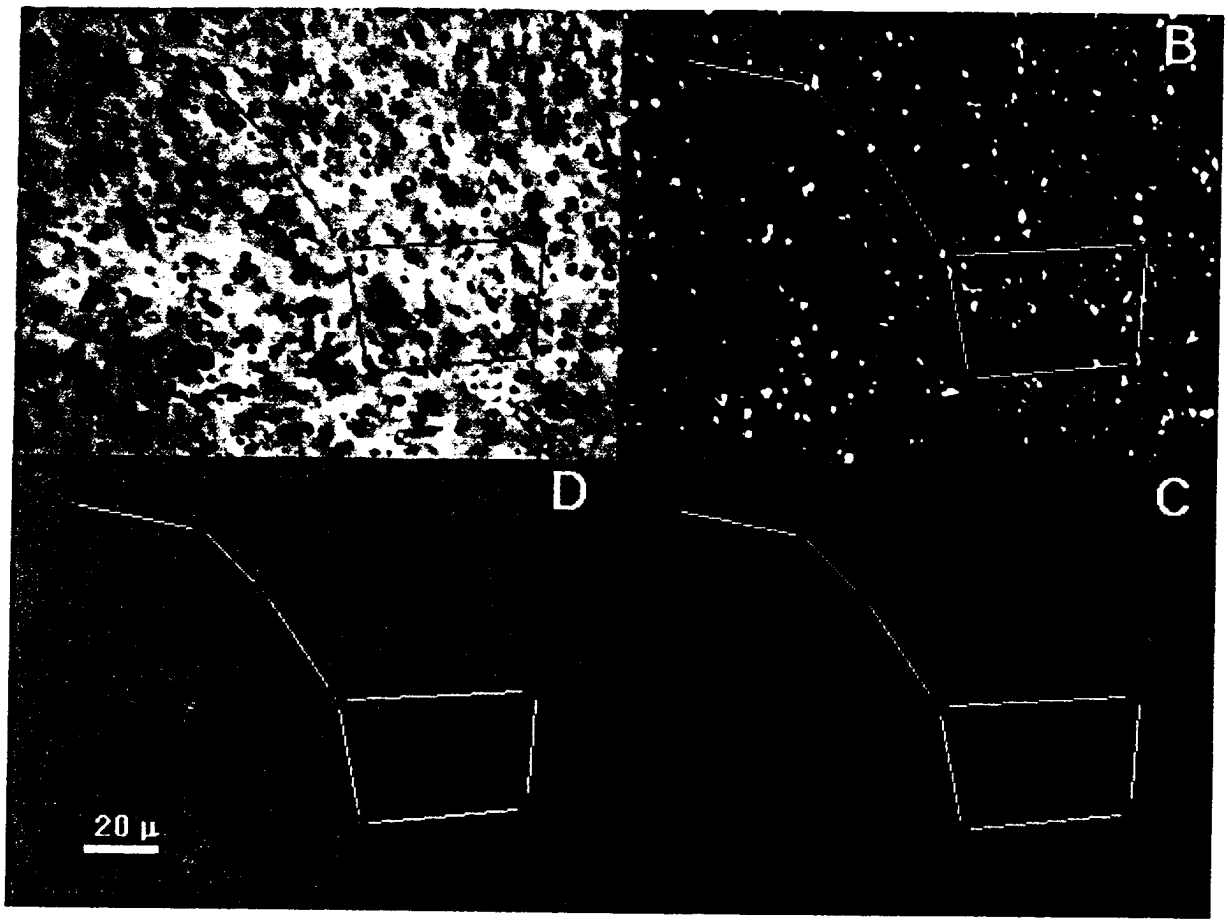

Figure 5. Light micrographs of DCA prepared with JPW1234 potentiometric dye and embedded into a PVA film: (A) general view; (B) one-photon scattering; (C) two-photon luminescence; and (D) two-photon (second harmonic, hyper Raleigh) scattering at 532 nm. The first two images, A and B, were obtained with ordinary white light illumination. The images C and D are obtained at 3 W cm^{-2} illumination by a Nd:YAG laser at 1.064 mm. No illumination in the visible was used for C and D. The image C is taken with a yellow filter cutting down emission at 532 nm completely and passing the yellow–red light. The image D is obtained with an 532 nm interference filter. In both cases, the residual infrared emission, scattered by the sample, was cut off by a special filter.

to the existence of an optimal coverage of a single colloidal particle by the dye which maximizes the light emission at the SH frequency.

We estimated experimentally the number of photons at 532 nm emitted by a single dye-coated silver colloidal particle illuminated by a Nd:YAG modelocked and Q-switched laser at a frequency of 400 Hz. It appeared that, at an average intensity of infrared illumination of only 3 W cm^{-2}, a particle of aggregated colloid with a mean diameter of 0.5 μm, containing about 120 small colloidal particles (unpublished data), emits over 720 SH photons per second. Such a signal is readily noticed in a light micrograph as a small point of light (see below).

To demonstrate the utility of aggregated dye-coated colloidal particles as a new kind of non-linear optical probe for light microscopy, we immobilized the particles prepared with JPW1234 potentiometric dye by inserting them into a polyvinyl alcohol (PVA) film. The sample was investigated using a light microscope equipped with a cooled CCD camera. A set of interchangeable color filters was used in order to view the sample at specific wavelengths. The typical micrographs of the probes distributed throughout a 0.2 mm-thick PVA film are shown in figure 5.

Image A gives the reader an idea of how a typical sample film looks. The black points are the DCAs. Image B is obtained in the dark field geometry. The white points in image B are DCAs which scatter light much more strongly than a PVA support. Images B and D display one- and two-photon scattering, while image C shows two-photon luminescence by the probes. In order to help the reader find correlations between positions of emitting probes, we connected the brightest points of the images with an imitation of the Big Dipper. It is seen that many of the probes seen as dark points in image A and/or as white points in image B, emit both green and yellow light as was expected based on the spectroscopic results described above. Thus, the results prove the unique utility of dye–colloid aggregates in non-linear optical microscopy with the use of a variety of non-linear optical processes.

As a next step towards utilizing the nanoantennae

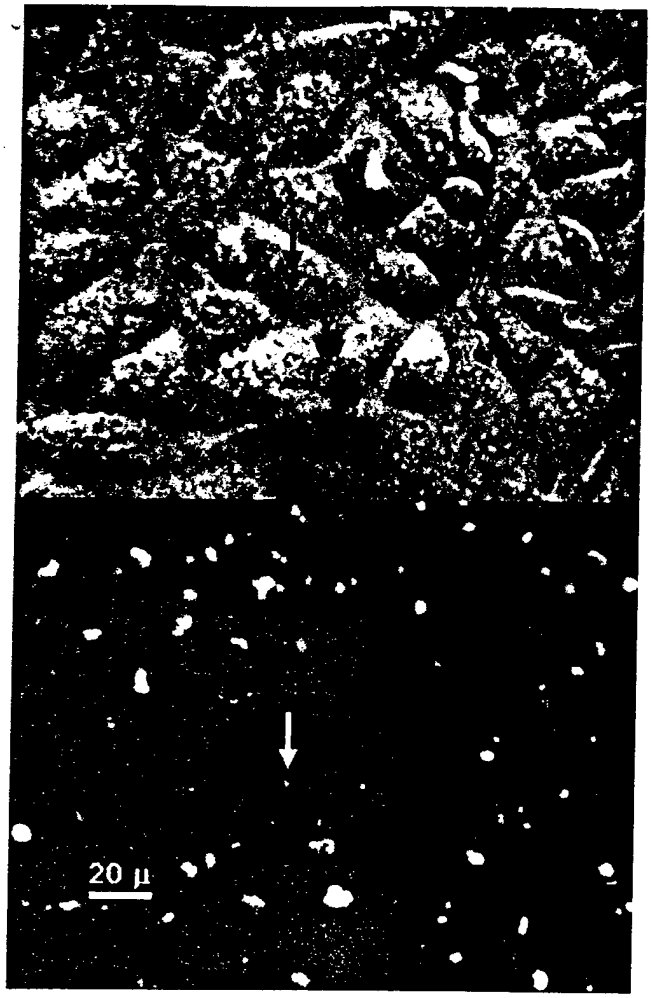

Figure 6. An experiment with a cell culture. Top, white light illumination. Bottom, infrared illumination with a Q-switched modelocked Nd:YAG laser at an average intensity of 3 W cm^{-2}.

probes in cellular microscopy, the probes were adsorbed to membranes of a cow corneal stromal cell culture. For this experiment, 50 μl of aqueous suspension of DCA, prepared with the JPW1234 potentiometric dye, was added to the culture dish. Within several minutes, the DCA sedimented onto the cell membranes.

The top part of figure 6, shows the general view of the probe covered cells. The probes are seen as dark spots. Since no monodispersion of probes was attempted at this stage, they had a variety of sizes and shapes. A black arrow in the top part of figure 6, points to a probe which is smaller than the wavelength of the light and so it is hardly seen in this figure. Subsequently, the white light illumination was turned off, and the sample was illuminated with a Nd:YAG laser emission at 1.06 μm. As in the previous experiment, an IR blocker was used to cut off any linearly scattered laser emission. The bottom part of figure 6 shows the picture taken by a CCD camera coupled to the microscope after several tens of seconds of exposure. The non-linear emission from the point probe marked with a black arrow

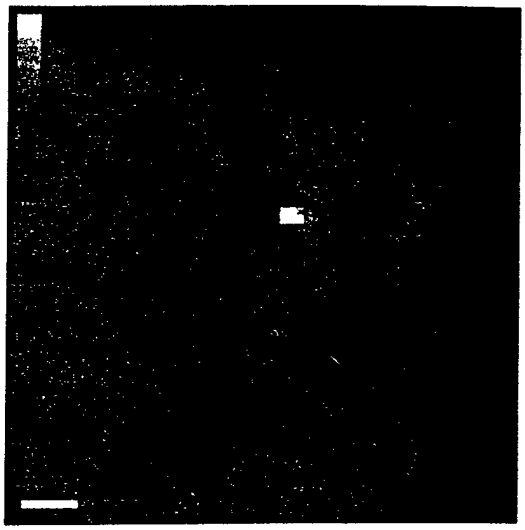

Figure 7. Dye stained P19 undifferentiated neuronal cells with nanodimension Ag microspheres resting on the labeled cell membrane. The white bar is 2μm and the colored bar represents a dynamic range of 0 to 256.

in the upper part of the figure is also seen as a bright point marked with white arrow at the bottom of figure 6. Thus, only emitting probes are seen with no background from the rest of the sample whatsoever.

3.1.3. Interaction of silver and gold nanocolloids with dye stained cell membranes. The local field enhancement of the silver microspheres relative to the background of the silver film was demonstrated in section 2.2 and in figure 1 in which the enhancement of these silver microspheres relative to the thin smooth silver film was evident. We have also extended these results on non-linear optical phenomena from these silver nanoparticles to dye stained cells on which are spread nanoparticles of silver. The dye used for these cell staining experiments was JPW1259 instead of JPW1234. The only difference in these dyes is in a non-conjugated substituent group attached to the non-linear chromophore [8]. Both of these dyes have hydrophobic carbon tails that very effectively anchor the dye with a specific orientation in a cell membrane, especially neuronal cell plasma membranes. The object in these dye stained cellular experiments was to detect an enhancement in the second harmonic generation of the dye which was embedded in the cell membrane and was in close proximity to the nanoparticle.

The SH image from a region of an undifferentiated P19 neuronal cell culture stained with JPW1259 and in contact with Ag nanoparticles is shown in figure 7. Once again, as in the case of the Ag microspheres on a thin metal film of silver, the region in which the microspheres are found is bright and the membrane bound dye over which there are no nanomicrospheres of Ag gives a very low background. Using the boxcar averager and channel integrator the absolute magnitude of the enhancement was

measured. A lower limit of this enhancement was one to two orders of magnitude in the SH signal intensity. Similar results were achieved with C2 muscle cells. Without the Ag microspheres the two-photon fluorescence from this same dye in these cells was approximately five times stronger than the second harmonic intensity while with the microspheres the enhanced dye second harmonic signal was as much as two fold stronger than the two-photon emission. This was similar to what was observed for these styryl dyes in the DCA experiments noted above.

As compared to our dye associated Ag colloids, and to the enhancement observed for pyridine on silver electrodes, [17], the relative enhancements we have observed for Ag microspheres interacting with stained membranes are several orders of magnitude lower. This could arise from several factors. First, the distance between the membrane bound dye and the silver microsphere was not optimized. This is crucial since there is a steep dependence on the magnitude of the signal as a function of distance [26]. This latter limitation is supported by the differences seen in the lower intensities that were needed to observe effects in the DCA nanoparticles relative to the situation that existed in the stained cell membranes on which the nanoparticles were resting. Second, the geometry of the particle is crucial in generating the maximum enhancement. The particles we used for the cellular experiments had a spherical rather than an elongated shape [26]. Thus, the particles were not optimally tuned for maximal enhancement at our wavelength. Furthermore, there were several factors in our experimental arrangement that led to lower detected enhancements in the cellular experiments. Specifically, the low magnification and low numerical aperture of the lens that was employed ($\times 50$ with NA $= 0.5$) in these experiments contributed significantly to the observation of the enhancement. Future research will be aimed at optimizing all these factors in order to get a maximal observed enhancement. The experiments reported in this paper clearly show that significant enhancement is possible in the non-linear optical phenomena we are observing. Calculations have shown that with optimized parameters enhancements can be as large as eight orders of magnitude [27].

The degree of interaction between dye and Ag microspheres when these microspheres are simply in contact with the stained membranes was investigated by comparing, under the same conditions, the SH signal from the Ag microspheres on a surface surrounded by a physiological medium without and with dye at a concentration that was used to stain the cells. In order to understand the results it is important to note that dye floating in the physiological medium and not in contact with the silver microspheres or the interface will not contribute a SH signal. Nonetheless, upon addition of dye we detected a several times increase in the SH signal from the pixels of the image that were directly associated with the nanoparticles. This was accomplished using a procedure that was described above to measure the magnitude of the relative enhancement of the Ag microspheres to the background. These results are consistent with the pyridine contribution to the signal from a roughened silver film [17]. As noted above in these results there was a 50 times increase in the silver enhancement due to the presence of the pyridine. Also, consistent with these results was the observation that the color of the microspheres on the slide was altered when the dye was introduced, in a manner that was consistent with what had been observed with the DCA particles in which the dye is physically complexed to the particle. Specifically, when the Ag microspheres were spread on a surface surrounded with physiological medium and zero dye concentration the microspheres appeared yellow–gold in color while the microspheres in contact with dye were brown to orange. This was similar to what was seen in the DCA spectra, see figure 3.

A variety of wavelengths were used to monitor the non-linear optical effects emanating from the regions of contact of the nanoparticles with a dye stained membrane. As in the case of the DCA nanoparticles we detected light at 532 nm which is due to SHG. This was shown by using the nearly quadratic dependence of the signal intensity as a function of the fundamental laser beam intensity. This is seen in figure 8 in which the second harmonic signal is plotted as a function of the square of the average radiated power. We also detected an emission at 610 nm probably arising from the two-photon fluorescence of the dye. An emission was also detected below 400 nm and this probably arises from some other multiphoton phenomenon that is as yet not fully understood. Below 400 nm the dependence of the emission on the fundamental laser power was more complicated in its functional dependence. Images at these three wavelengths are shown in figure 9 where it is clearly seen that the most significant enhancement is for the 532 nm SH wavelength. This is deduced from the relative signal to noise of the background where there are no microspheres to the regions where the microspheres are seen. For example compare the second harmonic image with the two-photon image seen in figure 9. As is clearly observed in these images the 532 nm emission in the region of the microsphere to the background is significantly higher than what is observed in the image at 610 nm. This is consistent with the spectral results and the results on the DCA shown both in terms of the emission spectra (figure 4) and the images that were obtained (figures 5 and 6). One probable factor relating to the higher background in the two-photon image is the fact that the aggregate of contributing molecules to this signal is considerably larger because of the lack of symmetry requirements in this third order process.

The results that we have obtained on all the dyes are consistent with a major contribution from field enhancement effects and not simply changes in the resonance behavior of the dye molecules as a result of their complexation with the metal particles. This is consistent with the observations of other workers [17, 28]. Such a deduction

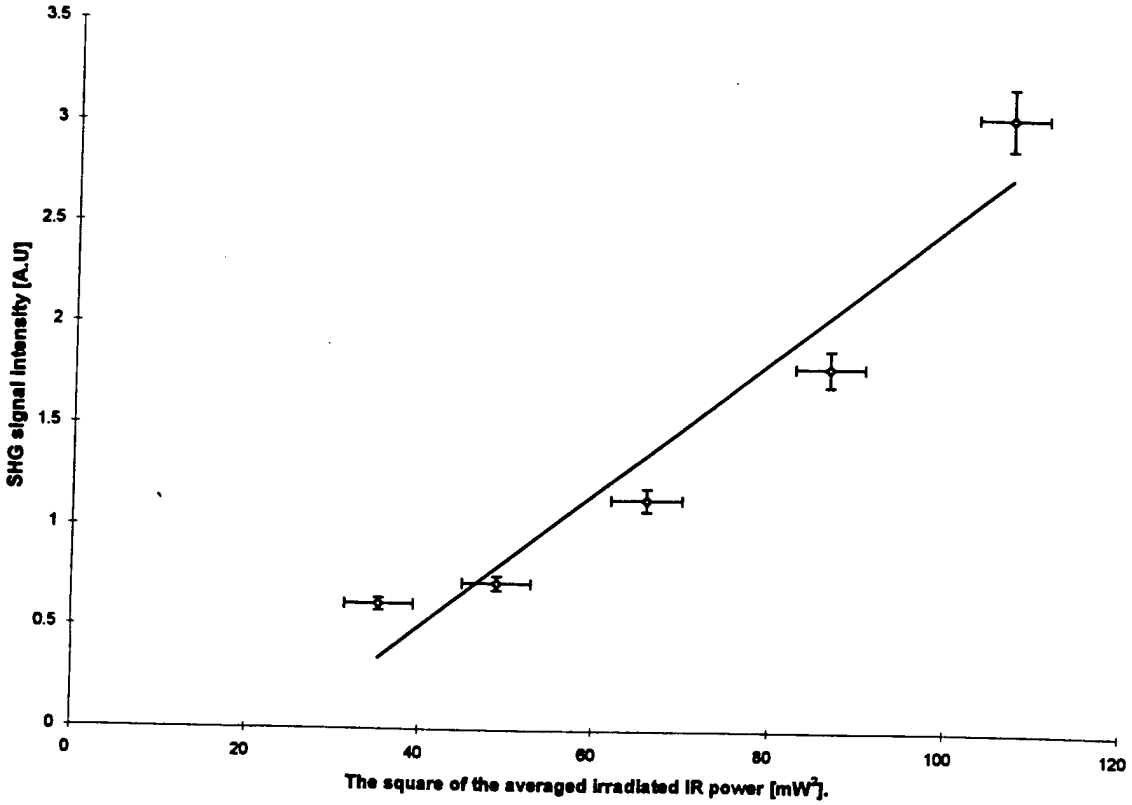

Figure 8. The second harmonic signal intensity as a function of the square of the average irradiated power at the fundamental wavelength. The *Y* axis is in arbitrary units and the *X* axis is in mW^2.

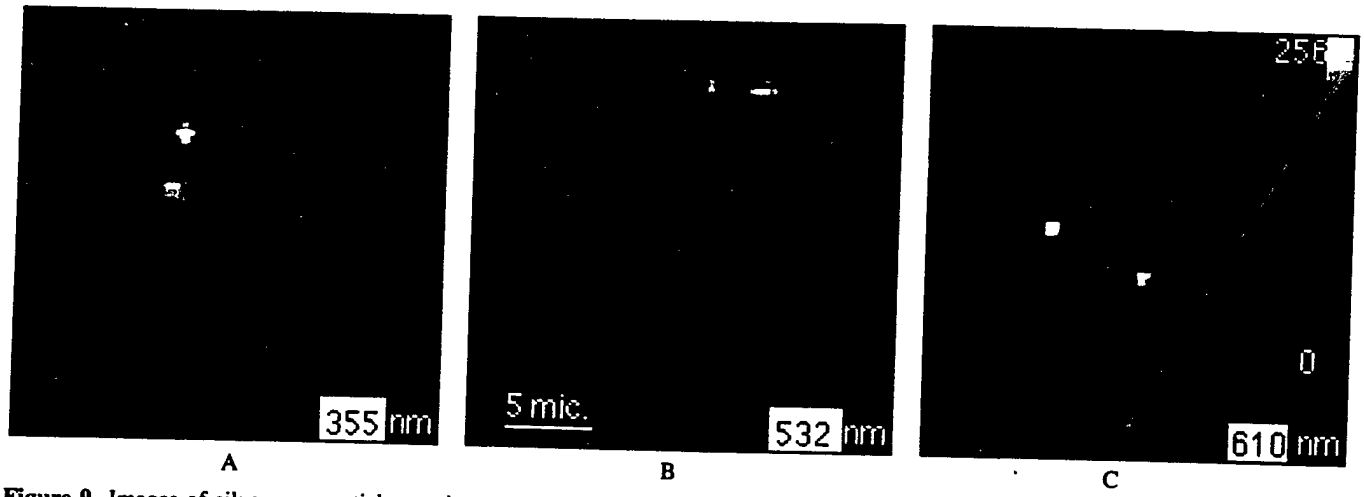

Figure 9. Images of silver nanoparticles resting on cell membranes of a P19 cell culture. The spectral imaging was accomplished at three different wavelengths associated with: A, multiphoton phenomena detected at 355 nm; B, second harmonic generation detected at 532 nm; and C, two-photon emission detected at 610 nm. Because the nanoparticles were not bound to the cell membrane and the sample was scanned to obtain the image the frames are not directly comparable.

can most clearly be seen in the emission behavior of the DCA particles all of which have approximately the same extinction at 532 nm with similar widths in the associated absorption spectra. Nonetheless, the relative enhancements that are obtained in the SH signal relative to the two-photon emission are significantly different in, for example, the Rhodamine 6G and the JPW dye. As noted above this arises from the alterations in the induced dipolar characteristics as a result of photon absorption that occurs for these dyes. The JPW has a very large induced dipole [7, 8] whereas the Rhodamine 6G is expected to have a dipole with a significantly reduced magnitude relative to JPW. Consistent